Error analysis of finite difference/collocation method for the nonlinear coupled parabolic free boundary problem modeling plaque growth in the artery

F. Nasresfahani · M. R. Eslahchi

Abstract The main target of this paper is to present a new and efficient method to solve a nonlinear free boundary mathematical model of atherosclerosis. This model consists of three parabolics, one elliptic and one ordinary differential equations that are coupled together and describe the growth of a plaque in the artery. We start our discussion by using the front fixing method to fix the free domain and simplify the model by changing the mix boundary condition to a Neumann one by applying suitable changes of variables. Then, after employing a nonclassical finite difference and the collocation method on this model, we prove the stability and convergence of methods. Finally, some numerical results are considered to show the efficiency of the method.

Keywords Spectral collocation method, Finite difference method, Nonlinear parabolic equation, Free boundary problem, Mathematical model, Atherosclerosis, Convergence and stability.

Mathematics Subject Classification (2010) 65M70, 65M12, 65M06, 35Q92, 35R35.

1 Introduction

There are many phenomena that we have questions about and want to describe them or their behaviours. To find an answer we collect data and multiple sources of data support a rapid knowledge.

Mohammad Reza Eslahchi, Corresponding author

eslahchi@modares.ac.ir

Farzaneh nasresfahani

f.nasresfahani@modares.ac.ir

Department of Applied Mathematics, Faculty of Mathematical Sciences, Tarbiat Modares University, P.O. Box 14115-134

Tehran, Iran

However, our ability to analyze and interpret this data lags far behind data generation and storage capacity. The question that arises here is how can mathematics help us to solve this problem? The answer to this question is that mathematics helps us in this issue by modeling as described in Figure 1 [33]. The first recognizable models were numbers since about 30.000 BC [41]. The development of mathematical models continued in various fields. By the invention of calculus by Newton and Leibniz in 1671, differential equations came into existence [34], and then, partial differential equations stand out in 1719 by Nicolaus Bernoulli [5]. Early 16th century was the beginning of the modern interaction between mathematics and biology duo to the work of William Harvey [24]. Thereafter, until the 20th century, biological modeling continued to advance by the work of Hardy in 1908 in population genetics [23], Yula in 1925 in birth and death process [48], Luria and Delbruck in 1943 in estimating bacterial mutation rates [31]. The question that matters here is what biological issues to biological scientists are more valuable and selected for modeling. In reply to the question, according to the authors' consideration, topics of the greatest importance to them are those that affect the human community more, which is the factor that causes a tendency to model for a more detailed examination of these issues. Due to human society conditions, studying diseases is the most important area of study. According to the ICD 10[1] [35], the most important diseases that cause of death in the world are HIV [10, 32], Tumor [9, 25, 37, 40], Cancer [2, 11, 17, 45], Cardiovascular diseases (especially Atherosclerosis) [6, 7, 13, 18, 22, 27, 47] and Wound healing [16, 28, 38, 46] respectively. As described above, the heart attack or stroke that happens because of atherosclerosis diseases is one of the third leading cause of death in the world [35]. There are two various perspectives to research in this area, "modeling" and "numerical analysis" point of view. In the case of modeling, the important point to note here is that there are different perspectives in studying Atherosclerosis [36, 42]. A very important perspective in the area of studying this disease is to study mathematical modeling in the forms of ordinary differential equation (ODE) and partial differential equation (PDE), that are distinguished from each other by the various factors such as choosing the region and the boundary, elements involved in biologically issues, boundary conditions and etc. For instance, in 2009 a 3-D nonlinear parabolic system of PDEs is considered as a mathematical model of Atherosclerosis involving the local blood flow dynamics by Calvez [6]. In 2010 Calvez extended his

---

[1] International Classification of Diseases

previous work [7]. In both articles, Calvez assumed the artery to be an irregular 3-D cylinder. Friedman in 2014, 2015 presented mathematical models of plaque growth in the artery, which parabolic nonlinear 2-D system of PDEs with mixed boundary conditions and free boundary are considered for modeling [19, 22]. It is worth noting that the difference between these models is that in [19] the artery is assumed to be a very long circular cylinder but in [22] the artery is considered as an irregular cylinder. In other work, a mathematical model with the approach used in [22] by including the effect of reverse cholesterol transport of plaque growth which includes the (LDL, HDL) concentrations is developed by Friedman [18]. There are many other models that are associated with this disease [13, 30, 47]. In the case of numerical analysis, there are various mathematical methods and different perspectives in convergence and stability analyzing. For instance, in [15] mathematical modeling of a tumor is considered and numerical results with convergence and stability of numerical methods have been presented. In [14] mathematical modeling of optimal control of tumor with drug application has been presented and in [15] it has been numerically solved and analyzed. Additionally, in [49], a two-dimensional multi-term time fractional diffusion equation is solved numerically using a fully-discrete schem and convergence and superconvergence of the method is illustrated. For the mathematical analysis point of view, in [39] a hyperbolic equation with an integral condition is solved using finite difference/spectral method.

In this article, we want to solve a free boundary nonlinear system of coupled PDEs that model Atherosclerosis and consists of three parabolics, one elliptic and one ordinary differential equation which is introduced in [19]. For the readers' convenience, we highlight the main goals of this study as follows

- We have fixed the domain using the front fixing method and simplified the model by changing the mix boundary condition to a Neumann one by applying a suitable change of variables to achieve more comfortable results for numerical analysis.
- Applying the finite difference method, we have constructed a sequence, which converges to the exact solution of coupled partial differential equations.
- In each time step, using Taylor theorem, the problem has changed to linear one (see (19)-(23)) and using the collocation method, equations (19)-(23) are solved numerically.
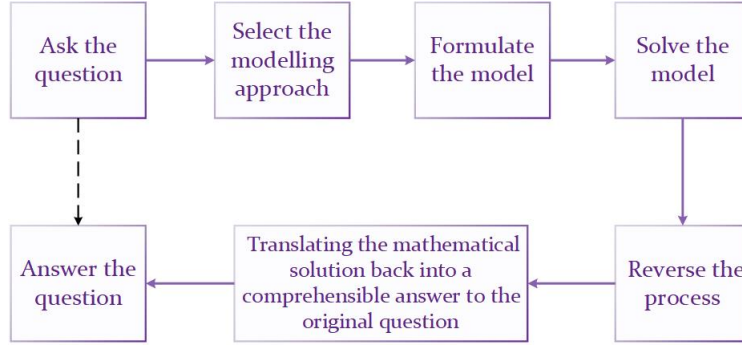
Fig. 1: *Seven steps to show the role of mathematical modeling in Solving the mathematical Problems [33].*

- We have proved constructed sequence converges to the exact solution of the problem (see Theorem 5.2) and also the stability of the method is proven (see Theorem 5.3).

- We have simulated the model using finite difference and collocation method for some pair of values (L_0, H_0) to show the validity and efficiency of the presented method. It is critical to note that, construction of a new second-order non-classical discretization formula helps us to prove the convergence and stability Theorem appropriately.

We organize our paper as follows: In Section 2, we introduce the model of Atherosclerosis presented by Friedman in [19]. We apply some changes to construct a more appropriate model for numerical and proof purposes in Section 3. In Section 4, we use finite difference and collocation method with convenience basis for approximating the solution of the problem. We discuss the stability and convergence of the method used for solving the model in Section 5. Finally, by presenting some numerical results, the theoretical statements are justified in Section 6.

2 Mathematical model

In this paper, we consider the following parabolic free boundary problem modeling plaque growth introduced in [19] as follows

$$\frac{\partial \widehat{L}}{\partial t} - \Delta \widehat{L} = -k_1 \frac{(M0 - \widehat{F})\widehat{L}}{K_1 + \widehat{L}} - r_1 \widehat{L}, \; R(t) < r < 1, \, t > 0,$$

$$\frac{\partial \widehat{L}}{\partial n} + \alpha(\widehat{L} - L_0) = 0, \; \text{at } r = R(t), \, t > 0, \quad \frac{\partial \widehat{L}}{\partial n} = 0, \; \text{at } r = 1, \, t > 0, \quad \widehat{L}(r,0) = L_0, \qquad (1)$$

$$\frac{\partial \widehat{H}}{\partial t} - \Delta \widehat{H} = -k_2 \frac{\widehat{H}\widehat{F}}{K_2 + \widehat{F}} - r_2\widehat{H}, \ R(t) < r < 1, \ t > 0,$$

$$\frac{\partial \widehat{H}}{\partial n} + \alpha(\widehat{H} - H_0) = 0, \ \text{at } r = R(t), \ t > 0, \quad \frac{\partial \widehat{H}}{\partial n} = 0, \ \text{at } r = 1, \ t > 0, \quad \widehat{H}(r,0) = H_0, \qquad (2)$$

$$\frac{\partial \widehat{F}}{\partial t} - D\Delta \widehat{F} + \widehat{F}_r.v = k_1 \frac{(M_0 - \widehat{F})\widehat{L}}{K1 + \widehat{L}} - k_2 \frac{\widehat{H}\widehat{F}}{K_2 + \widehat{F}} -$$

$$\lambda \frac{\widehat{F}(M_0 - \widehat{F})\widehat{L}}{M_0(\delta + \widehat{H})} + \frac{\mu_1}{M_0}(M_0 - \widehat{F})\widehat{F} - \frac{\mu_2}{M_0}\widehat{F}(M_0 - \widehat{F}), \ R(t) < r < 1, \ t > 0,$$

$$\frac{\partial \widehat{F}}{\partial n} + \beta \widehat{F} = 0 \quad , \ \text{at } r = R(t), \ t > 0, \quad \frac{\partial \widehat{F}}{\partial n} = 0 \quad , \ \text{at } r = 1, \ t > 0, \quad F(r,0) = 0, \qquad (3)$$

$$M_0.v_r = \lambda \frac{(M_0 - \widehat{F})\widehat{L}}{\delta + \widehat{H}} - \mu_1(M_0 - \widehat{F}) - \mu_2\widehat{F}, \ R(t) < r < 1, \ t > 0,$$

$$v(r,t) = 0, \ \text{at } r = 1, \ t > 0, \qquad (4)$$

$$\frac{dR(t)}{dt} = v(R(t),t), \ t > 0,$$

$$R(0) = \epsilon. \qquad (5)$$

There are several mathematical models that describe the growth of a plaque in the artery. All these models recognize the critical role of the bad cholesterols and the good cholesterols in determining whether a plaque, once formed, will grow or shrink.

In mathematical models, choosing the type of geometry of the problem is very important. Since the plaques grown in the artery are approximately spherically symmetric, in most of the models, it is assumed that the plaque grows radially-symmetric. In this model, it is assumed that the artery is a very long circular cylinder and a circular cross-section $0 \leq r \leq 1$ is considered. The plaque is given by $R(t) < r < 1$, where r is measured in unit of cm, and t is measured in unit of days. Also, The variables $\widehat{L}$, $\widehat{H}$ and $\widehat{F}$ are taken to be functions of (r,t) only in the region $\{(r,t); R(t) < r < 1, t > 0\}$. In this model, $\widehat{L}$, $\widehat{H}$ and $\widehat{F}$ are the variables that illustrate the concentration of LDL and HDL and the density of foam cell in the plaque respectively and v is the radial velocity. k_1 is the rate of ox-LDL ingestion by macrophages. k_2 is the rate of reverse cholesterol transport. r_1 and r_2 represent the degradation of the LDL and HDL caused by radicals respectively. μ_1 and μ_2 are the death rate of macrophages and foam cells respectively. Also, D is the diffusion coefficients of foam cells. Initially, in order to better understand the model, it is better to know a little how the plaque is calcified in the artery. A plaque contains low density lipoprotein (LDL) or bad cholesterol, high-density lipoprotein (HDL) or good
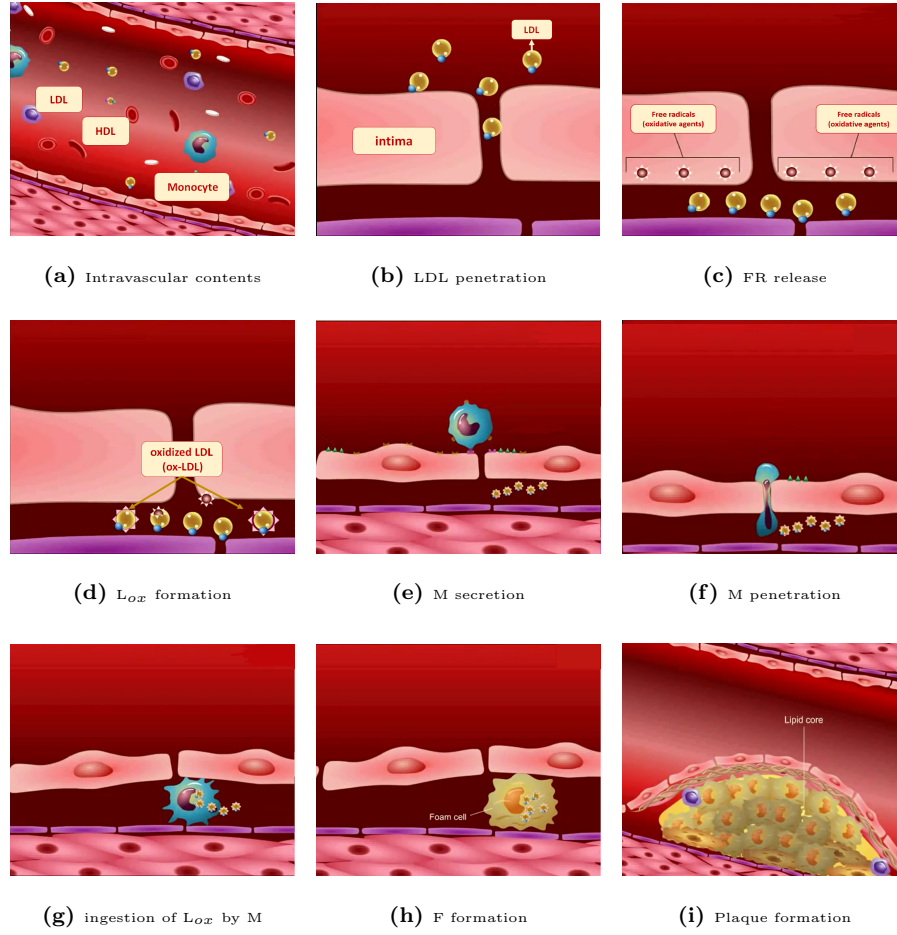
(a) Intravascular contents

(b) LDL penetration

(c) FR release

(d) L_{ox} formation

(e) M secretion

(f) M penetration

(g) ingestion of L_{ox} by M

(h) F formation

(i) Plaque formation

Fig. 2: *The process of plaque development [1].*

cholesterol, macrophages and foam cells (Figure 2.a). The process of plaque development begins with a lesion in the endothelial layer, penetration of low density lipoproteins in the intima (Figure 2.b) and by Free radicals in the initma (Figure 2.c) becoming oxidized LDL (Figure 2.d) and it is presented in the second term of (1). Notice that in this model $\widehat{L}$ (and $\widehat{H}$) and its oxidized form $\widehat{L}_{ox}$ (and $\widehat{H}_{ox}$) are merged. Free radicals are oxidative agents continuously released by biochemical reactions within the body, including the intima [3, 44]. Endothelial cells, sensing the presence of ox-LDL, are activated and trigger monocyte chemoattractant protein, which triggers recruitment of monocytes into the intima (Figure 2.e) [3,21]. After entering the intima, monocytes differentiate into macrophages (M) (Figure 2.f). The ingestion of large amounts of ox-LDL (Figure 2.g), that shown in the first term of (1), transforms the fatty macrophages into the foam cells (Figure 2.h) [4]. Newly formed foam cells secrete chemokines which attract more macrophages, and the plaque is gradually calcified (Figure 2.i). At the same time

that LDL enters the intima, high-density lipoprotein also enters the intima and becomes oxidized by free radicals (FR) as presented by the second term of (2). However, oxidized HDL (H_{ox}) is not ingested by macrophages. HDL helps to prevent Atherosclerosis by removing cholesterol from foam cells, and by the limiting inflammatory processes that underline Atherosclerosis, as shown in the first term of (2). Furthermore, HDL takes up free radicals that are otherwise available to LDL [22]. As the plaque continues to grow (Figure 2.i), the increased shear force may cause rupture of the plaque, possibly resulting in the formation of a thrombus (blood clot) and heart attack (for more information about the model see [19]).

For simplicity, we consider the model from cylindrical coordinates (1)-(5) to spherical coordinates as follows

$$\frac{\partial \widehat{L}}{\partial t} - \frac{1}{r^2}\frac{\partial}{\partial r}(r^2\frac{\partial \widehat{L}}{\partial r}) = -k_1\frac{(M_0 - \widehat{F})\widehat{L}}{K_1 + \widehat{L}} - r_1\widehat{L}, \; R(t) < r < 1, \, t > 0,$$

$$\frac{\partial \widehat{L}}{\partial r} + \alpha(\widehat{L} - L_0) = 0 \text{ at } r = R(t), \, t > 0, \quad \frac{\partial \widehat{L}}{\partial r} = 0 \text{ at } r = 1, \, t > 0, \quad \widehat{L}(r,0) = L_0, \tag{6}$$

$$\frac{\partial \widehat{H}}{\partial t} - \frac{1}{r^2}\frac{\partial}{\partial r}(r^2\frac{\partial \widehat{H}}{\partial r}) = -k_2\frac{\widehat{H}\widehat{F}}{K_2 + \widehat{F}} - r_2\widehat{H}, \; R(t) < r < 1, \, t > 0,$$

$$\frac{\partial \widehat{H}}{\partial r} + \alpha(\widehat{H} - H_0) = 0 \text{ at } r = R(t), \, t > 0, \quad \frac{\partial \widehat{H}}{\partial r} = 0 \text{ at } r = 1, \, t > 0, \quad \widehat{H}(r,0) = H_0, \tag{7}$$

$$\frac{\partial \widehat{F}}{\partial t} - \frac{D}{r^2}\frac{\partial}{\partial r}(r^2\frac{\partial \widehat{F}}{\partial r}) + \widehat{F}_r.v = k_1\frac{(M_0 - \widehat{F})\widehat{L}}{K1 + \widehat{L}} - k_2\frac{\widehat{H}\widehat{F}}{K_2 + \widehat{F}} -$$

$$\lambda\frac{\widehat{F}(M_0 - \widehat{F})\widehat{L}}{M_0(\delta + \widehat{H})} + \frac{\mu_1}{M_0}(M_0 - \widehat{F})\widehat{F} - \frac{\mu_2}{M_0}\widehat{F}(M_0 - \widehat{F}), \; R(t) < r < 1, \, t > 0,$$

$$\frac{\partial \widehat{F}}{\partial r} + \beta\widehat{F} = 0 \text{ at } R(t) < r < 1, \, t > 0, \quad \frac{\partial \widehat{F}}{\partial r} = 0 \text{ at } r = 1, \, t > 0, \quad \widehat{F}(r,0) = 0, \tag{8}$$

$$M_0.v_r = \lambda\frac{(M_0 - \widehat{F})\widehat{L}}{\delta + \widehat{H}} - \mu_1(M_0 - \widehat{F}) - \mu_2\widehat{F}, \; R(t) < r < 1, \, t > 0,$$

$$v(r,t) = 0 \text{ at } r = 1, \, t > 0, \tag{9}$$

$$\frac{dR(t)}{dt} = v(R(t),t), \, t > 0,$$

$$R(0) = \epsilon. \tag{10}$$

In the next section, we want to present a new reformulation of the model presented in (6)-(10).

3 A new reformulation of the model

Most of the mathematical models that originate from biological phenomena have some special features. Free or moving boundary condition, mix (robin) boundary condition and many other features of a mathematical model can cause some difficulties in applying classical numerical methods on them and researchers overcome these difficulties by applying suitable techniques. Since the model of Atherosclerosis (6)-10) is a free boundary model with mix boundary condition, to solve this model numerically, we need to remove the mentioned difficulties. To reach this aim, we must consider a new reformulation of this model for which the free boundary change to a fixe one and the robin (mix) boundary condition change to a Neumann one.

3.1 Fixing the domain

Due to the fact that the plaque grows radially symmetric with free boundary, using the front fixing method by the following variable changes

$$\rho = \frac{r - R(t)}{1 - R(t)}, \quad \widehat{L}(\rho, t) = \widehat{L}(r, t), \ \widehat{H}(\rho, t) = \widehat{H}(r, t), \ \widehat{F}(\rho, t) = \widehat{F}(r, t),$$

the free boundary problem (6)-(10) is transformed into a problem with a fixed domain

$$\{(\rho, t) \mid 0 < \rho < 1, t \geq 0\},$$

and the model becomes as follows

$$\frac{\partial \widehat{L}}{\partial t} - \frac{1}{(1 - R(t))^2} \frac{\partial^2 \widehat{L}}{\partial \rho^2} + \left(\frac{-2}{\rho(1 - R(t))^2 + R(t)(1 - R(t))} + \frac{v(0, t)(\rho - 1)}{(1 - R(t))^2} \right) \frac{\partial \widehat{L}}{\partial \rho} = f^{\widehat{L}}(\widehat{L}, \widehat{F}),$$

$$\frac{\partial \widehat{L}}{\partial \rho} + \alpha(1 - R(t))(\widehat{L} - L_0) = 0 \text{ at } \rho = 0, \ t > 0, \quad \frac{\partial \widehat{L}}{\partial \rho} = 0 \text{ at } \rho = 1, \ t > 0, \quad \widehat{L}(\rho, 0) = L_0, \quad (11)$$

$$\frac{\partial \widehat{H}}{\partial t} - \frac{1}{(1 - R(t))^2} \frac{\partial^2 \widehat{H}}{\partial \rho^2} + \left(\frac{-2}{\rho(1 - R(t))^2 + R(t)(1 - R(t))} + \frac{v(0, t)(\rho - 1)}{(1 - R(t))^2} \right) \frac{\partial \widehat{H}}{\partial \rho} = f^{\widehat{H}}(\widehat{H}, \widehat{F}),$$

$$\frac{\partial \widehat{H}}{\partial \rho} + \alpha(1 - R(t))(\widehat{H} - H_0) = 0 \text{ at } \rho = 0, \ t > 0, \quad \frac{\partial \widehat{H}}{\partial \rho} = 0 \text{ at } \rho = 1, \ t > 0, \quad \widehat{H}(\rho, 0) = H_0, \quad (12)$$

$$\frac{\partial \widehat{F}}{\partial t} - \frac{D}{(1 - R(t))^2} \frac{\partial^2 \widehat{F}}{\partial \rho^2} +$$

$$\left(\frac{-2D}{\rho(1 - R(t))^2 + R(t)(1 - R(t))} + \frac{v}{1 - R(t)} + \frac{v(0, t)(\rho - 1)}{(1 - R(t))^2} \right) \frac{\partial \widehat{F}}{\partial \rho} = f^{\widehat{F}}(\widehat{L}, \widehat{H}, \widehat{F}),$$

$$\frac{\partial \widehat{F}}{\partial \rho} + \beta(1 - R(t))\widehat{F} = 0 \text{ at } \rho = 0, \ t > 0, \quad \frac{\partial \widehat{F}}{\partial \rho} = 0 \text{ at } \rho = 1, \ t > 0, \quad \widehat{F}(\rho, 0) = 0, \quad (13)$$

$$\frac{1}{1 - R(t)}\frac{\partial v}{\partial \rho} = f^v(\widehat{L}, \widehat{H}, \widehat{F}),$$

$$v(\rho, t) = 0 \text{ at } \rho = 1, \, t > 0, \tag{14}$$

$$\frac{dR}{dt} = v(0, t), \, t > 0,$$

$$R(0) = \epsilon. \tag{15}$$

3.2 changing the boundary condition

To obtain more comfortable results for numerical analysis, without loss of generality, we can change the mixed boundary condition of the model to a Neumann one by applying suitable variable changes as follows

$$L(\rho, t) := \exp(-\alpha(1 - R(t))\frac{(1 - \rho)^2}{2})(\widehat{L}(\rho, t) - L_0), \tag{16}$$

$$H(\rho, t) := \exp(-\alpha(1 - R(t))\frac{(1 - \rho)^2}{2})(\widehat{H}(\rho, t) - H_0), \tag{17}$$

$$F(\rho, t) := \exp(-\beta(1 - R(t))\frac{(1 - \rho)^2}{2})\widehat{F}(\rho, t). \tag{18}$$

So, from (11)-(15) we have

$$\frac{\partial L}{\partial t} - \frac{1}{(1 - R(t))^2}\frac{\partial^2 L}{\partial \rho^2} +$$
$$\left(\frac{-2}{\rho(1 - R(t))^2 + R(t)(1 - R(t))} + \frac{v(0, t)(\rho - 1)}{1 - R(t)} + \frac{2(1 - \rho)\alpha}{1 - R(t)}\right)\frac{\partial L}{\partial \rho} = f^L(L, F),$$
$$\frac{\partial L}{\partial \rho} = 0 \text{ at } \rho = 0, \, t > 0, \quad \frac{\partial L}{\partial \rho} = 0 \text{ at } \rho = 1, \, t > 0, \quad L(\rho, 0) = 0, \tag{19}$$

$$\frac{\partial H}{\partial t} - \frac{1}{(1 - R(t))^2}\frac{\partial^2 H}{\partial \rho^2} +$$
$$\left(\frac{-2}{\rho(1 - R(t))^2 + R(t)(1 - R(t))} + \frac{v(0, t)(\rho - 1)}{1 - R(t)} + \frac{2(1 - \rho)\alpha}{1 - R(t)}\right)\frac{\partial H}{\partial \rho} = f^H(H, F),$$
$$\frac{\partial H}{\partial \rho} = 0 \text{ at } \rho = 0, \, t > 0, \quad \frac{\partial H}{\partial \rho} = 0 \text{ at } \rho = 1, \, t > 0, \quad H(\rho, 0) = 0, \tag{20}$$

$$\frac{\partial F}{\partial t} - \frac{D}{(1 - R(t))^2}\frac{\partial^2 F}{\partial \rho^2} +$$
$$\left(\frac{-2D}{\rho(1 - R(t))^2 + R(t)(1 - R(t))} + \frac{v}{1 - R(t)} + \frac{v(0, t)(\rho - 1)}{1 - R(t)} + \frac{2D(1 - \rho)\beta}{1 - R(t)}\right)\frac{\partial F}{\partial \rho} = f^F(L, H, F)$$
$$\frac{\partial F}{\partial \rho} = 0 \text{ at } \rho = 0, \, t > 0, \quad \frac{\partial F}{\partial \rho} = 0 \text{ at } \rho = 1, \, t > 0, \quad F(\rho, 0) = 0, \tag{21}$$

$$\frac{1}{1 - R(t)} \frac{\partial v}{\partial \rho} = f^v(L, H, F),$$

$$v(\rho, t) = 0 \text{ at } \rho = 1, \ t > 0, \tag{22}$$

$$\frac{dR}{dt} = v(0, t), \ t > 0,$$

$$R(0) = \epsilon. \tag{23}$$

4 Approximating the solution of the problem

In this section, we approximate the solution of the problem (19)-(23) for $0 < \rho < 1$ and $0 < t < T$. Let $t_i := ih$ $(i = 0, 1, \ldots, M)$ be mesh points, where $h := \dfrac{T}{M}$ is the time step and M is a positive integer. The problem is solved using the finite difference-collocation method. In order to prove the stability and convergence of the method, we need to construct a non-classical discretization of second-order to approximate the time derivative. So, let us consider the following discretization formula for approximating the time derivative for a given function $u(\rho, t)$

$$\frac{\partial u}{\partial t}(\rho, t_{n+1}) = \frac{u_{n+1} - u_n + \dfrac{u_{n-1} - u_n}{3}}{\dfrac{2h}{3}} + E_t, \tag{24}$$

and the following approximation formula for linearizing the equations

$$u(\rho, t_{n+1}) = 2u(\rho, t_n) - u(\rho, t_{n-1}) + E^u, \tag{25}$$

where

$$\max\{\|E_t\|_\infty, \|E^u\|_\infty\} < Ch^2, \tag{26}$$

and C is a positive constant. In the following, we have assumed that

$$u_n(\rho) = u(\rho, t_n).$$

Using finite difference method based on the approximation formula given by (24) and equations (11)-(13) we get

$$L_{n+1} - L_n + \frac{L_{n-1} - L_n}{3} - \frac{2h}{3(1 - R_{n+1})^2} \frac{\partial^2 L_{n+1}}{\partial \rho^2} +$$
$$\frac{2h}{3} \left(\frac{-2}{\rho(1 - R_{n+1})^2 + R_{n+1}(1 - R_{n+1})} + \frac{(2v_n(0) - v_{n-1}(0))(\rho - 1)}{1 - R_{n+1}} + \frac{2(1 - \rho)\alpha}{1 - R_{n+1}} \right) \frac{\partial L_{n+1}}{\partial \rho} =$$
$$\frac{2h}{3} (2f^L(L_n, F_n) - f^L(L_{n-1}, F_{n-1})) - \frac{2h}{3} E_t^L,$$

$$\frac{\partial L_{n+1}}{\partial \rho} = 0 \text{ at } \rho = 0, \ t > 0, \quad \frac{\partial L_{n+1}}{\partial \rho} = 0 \text{ at } \rho = 1, \ t > 0, \quad L_0(\rho) = 0,$$

$$H_{n+1} - H_n + \frac{H_{n-1} - H_n}{3} - \frac{2h}{3(1 - R_{n+1})^2} \frac{\partial^2 H_{n+1}}{\partial \rho^2} +$$

$$\frac{2h}{3} \left(\frac{-2}{\rho(1 - R_{n+1})^2 + R_{n+1}(1 - R_{n+1})} + \frac{(2v_n(0) - v_{n-1}(0))(\rho - 1)}{1 - R_{n+1}} + \frac{2(1 - \rho)\alpha}{1 - R_{n+1}} \right) \frac{\partial H_{n+1}}{\partial \rho} =$$

$$\frac{2h}{3}(2f^H(H_n, F_n) - f^H(H_{n-1}, F_{n-1})) - \frac{2h}{3} E_t^H,$$

$$\frac{\partial H_{n+1}}{\partial \rho} = 0 \text{ at } \rho = 0,\ t > 0, \quad \frac{\partial H_{n+1}}{\partial \rho} = 0 \text{ at } \rho = 1,\ t > 0, \quad H_0(\rho) = 0,$$

$$F_{n+1} - F_n + \frac{F_{n-1} - F_n}{3} - \frac{2hD}{3(1 - R_{n+1})^2} \frac{\partial^2 F_{n+1}}{\partial \rho^2} +$$

$$\frac{2h}{3} \left(\frac{-2D}{\rho(1 - R_{n+1})^2 + R_{n+1}(1 - R_{n+1})} + \frac{(2v_n - v_{n-1})}{1 - R_{n+1}} + \right.$$

$$\left. \frac{(2v_n(0) - v_{n-1}(0))(\rho - 1)}{1 - R_{n+1}} + \frac{2D(1 - \rho)\beta}{1 - R_{n+1}} \right) \frac{\partial F_{n+1}}{\partial \rho} =$$

$$\frac{2h}{3}(2f^F(L_n, H_n, F_n) - f^F(L_{n-1}, H_{n-1}, F_{n-1})) - \frac{2h}{3} E_t^F,$$

$$\frac{\partial F_{n+1}}{\partial \rho} = 0 \text{ at } \rho = 0,\ t > 0, \quad \frac{\partial F_{n+1}}{\partial \rho} = 0 \text{ at } \rho = 1,\ t > 0, \quad F_0(\rho) = 0, \tag{27}$$

$$\frac{1}{1 - R_n} \frac{\partial v_n}{\partial \rho} = f^v(L_n, H_n, F_n),$$

$$v(\rho, t) = 0 \text{ at } \rho = 1,\ t > 0, \tag{28}$$

where E_t^u is obtained by merging the errors of E_t and E^u. From (26), there exists positive C^* such that

$$\max\{\|E_t^L\|_\infty, \|E_t^H\|_\infty, \|E_t^F\|_\infty\} < C^* h^2, \tag{29}$$

and using (15) we have

$$R_{n+1} = R_n - \frac{R_{n-1} - R_n}{h} + 2hv_n(0) - \frac{2h}{3} E_t^R. \tag{30}$$

Then, we conclude that there exists positive constant C^{**} such that

$$max\{\|E_t^L\|_\infty, \|E_t^H\|_\infty, \|E_t^F\|_\infty, \|E_t^R\|_\infty\} < C^{**} h^2. \tag{31}$$

In the rest of this paper, the solution of the problem (6)-(7) is denoted by $(L_{n+1}^{ap}, H_{n+1}^{ap}, F_{n+1}^{ap})$, which

is the approximated solution of the following problem

$$L_{n+1} - \frac{h^*}{(1 - R_{n+1}^{ap})^2} \frac{\partial^2 L_{n+1}}{\partial \rho^2} +$$

$$h^* \left(\frac{-2}{\rho(1 - R_{n+1}^{ap})^2 + R_{n+1}^{ap}(1 - R_{n+1}^{ap})} + \frac{(2v_n^{ap}(0) - v_{n-1}^{ap}(0))(\rho - 1)}{1 - R_{n+1}^{ap}} + \frac{2(1 - \rho)\alpha}{1 - R_{n+1}^{ap}} \right) \frac{\partial L_{n+1}}{\partial \rho} =$$

$$h^*(2f^L(L_n^{ap}, F_n^{ap}) - f^L(L_{n-1}^{ap}, F_{n-1}^{ap})) + L_n^{ap} - \frac{L_{n-1}^{ap} - L_n^{ap}}{3},$$

$$\frac{\partial L_{n+1}}{\partial \rho} = 0 \text{ at } \rho = 0,\ t > 0, \quad \frac{\partial L_{n+1}}{\partial \rho} = 0 \text{ at } \rho = 1,\ t > 0, \quad L_0(\rho) = 0, \tag{32}$$

$$H_{n+1} - \frac{h^*}{(1-R_{n+1}^{ap})^2}\frac{\partial^2 H_{n+1}}{\partial\rho^2} +$$

$$h^*\left(\frac{-2}{\rho(1-R_{n+1}^{ap})^2 + R_{n+1}^{ap}(1-R_{n+1}^{ap})} + \frac{(2v_n^{ap}(0) - v_{n-1}^{ap}(0))(\rho-1)}{1-R_{n+1}} + \frac{2(1-\rho)\alpha}{1-R_{n+1}^{ap}}\right)\frac{\partial H_{n+1}}{\partial\rho} =$$

$$h^*(2f^H(H_n^{ap}, F_n^{ap}) - f^H(H_{n-1}^{ap}, F_{n-1}^{ap})) + H_n^{ap} - \frac{H_{n-1}^{ap} - H_n^{ap}}{3},$$

$$\frac{\partial H_{n+1}}{\partial\rho} = 0 \text{ at } \rho = 0,\ t > 0, \quad \frac{\partial H_{n+1}}{\partial\rho} = 0 \text{ at } \rho = 1,\ t > 0, \quad H_0(\rho) = 0, \qquad (33)$$

$$F_{n+1} - \frac{h^*D}{(1-R_{n+1}^{ap})^2}\frac{\partial^2 F_{n+1}}{\partial\rho^2} +$$

$$h^*\left(\frac{-2D}{\rho(1-R_{n+1}^{ap})^2 + R_{n+1}^{ap}(1-R_{n+1}^{ap})} + \frac{(2v_n^{ap} - v_{n-1}^{ap})}{1-R_{n+1}^{ap}}\right.$$

$$\left. + \frac{(2v_n^{ap}(0) - v_{n-1}^{ap}(0))(\rho-1)}{1-R_{n+1}^{ap}} + \frac{2D(1-\rho)\beta}{1-R_{n+1}^{ap}}\right)\frac{\partial F_{n+1}}{\partial\rho} =$$

$$h^*(2f^F(L_n^{ap}, H_n^{ap}, F_n^{ap}) - f^F(L_{n-1}^{ap}, H_{n-1}^{ap}, F_{n-1}^{ap})) + F_n^{ap} - \frac{F_{n-1}^{ap} - F_n^{ap}}{3},$$

$$\frac{\partial F_{n+1}}{\partial\rho} = 0 \text{ at } \rho = 0,\ t > 0, \quad \frac{\partial F_{n+1}}{\partial\rho} = 0 \text{ at } \rho = 1,\ t > 0, \quad F_0(\rho) = 0, \qquad (34)$$

$$\frac{1}{1-R_{n+1}^{ap}}\frac{\partial v_n^{ap}}{\partial\rho} = f^v(L_n^{ap}, H_n^{ap}, F_n^{ap}),$$

$$v(\rho, t) = 0 \text{ at } \rho = 1,\ t > 0, \qquad (35)$$

$$R_{n+1}^{ap} = R_n^{ap} - \frac{R_{n-1}^{ap} - R_n^{ap}}{3} + h^*v_n^{ap}(0), \qquad (36)$$

where $h^* = \frac{2h}{3}$ and $(L_{n+1}^{ap}, H_{n+1}^{ap}, F_{n+1}^{ap})$ is obtained as an approximation of $(L_{n+1}, H_{n+1}, F_{n+1})$ by solving (32)-(36) employing the collocation method. To implement this method, we employ $\{p_i(\rho)\}_{i=0}^{\infty}$ as trial functions as follows

$$\text{span}\{p_0(\rho), p_1(\rho), ..., p_k(\rho)\} = \{u \in \text{span}\{1, \rho, \rho^2, ..., \rho^{k+2}\};\ \frac{\partial u}{\partial\rho}|_{\rho=0} = 0,\ \frac{\partial u}{\partial\rho}|_{\rho=1} = 0\}. \qquad (37)$$

Then, we approximate F_{n+1} by F_{n+1}^N defined as follows

$$F_{n+1}^N(\rho) = \sum_{i=0}^{N} a_i^{n+1} p_i(\rho). \qquad (38)$$

Now, we consider the following equation

$$\Pi_N^{0,0} F_{n+1}^N - \frac{h^*D}{(1-R_{n+1}^{ap})^2}\Pi_N^{0,0}\frac{\partial^2 F_{n+1}^N}{\partial\rho^2} + h^*\Pi_N^{0,0}(G(\rho)\frac{\partial F_{n+1}^N}{\partial\rho}) = I_N^{0,0} g_n^*, \qquad (39)$$

where

$$g_n^* = \Pi_N^{0,0}\left(F_n^{ap} - \frac{F_{n-1}^{ap} - F_n^{ap}}{3}\right) + \underbrace{h^*(2f^F(L_n^{ap}, H_n^{ap}, F_n^{ap}) - f^F(L_{n-1}^{ap}, H_{n-1}^{ap}, F_{n-1}^{ap}))}_{f_n^*}, \qquad (40)$$

and

$$G(\rho) = \frac{-2D}{\rho(1 - R_{n+1}^{ap})^2 + R_{n+1}^{ap}(1 - R_{n+1}^{ap})} +$$

$$\frac{(2v_n^{ap} - v_{n-1}^{ap})}{1 - R_{n+1}^{ap}} + \frac{(2v_n^{ap}(0) - v_{n-1}^{ap}(0))(\rho - 1)}{1 - R_{n+1}^{ap}} + \frac{2D(1 - \rho)\beta}{1 - R_{n+1}^{ap}}, \tag{41}$$

where $\Pi_N^{0,0}$ and $I_N^{0,0}$ are the orthogonal projection and Jacobi-Gauss-Lobatto interpolation operator with respect to ρ on $[0, 1]$, respectively. The approximation of the solution of (32) and (33) can be obtained by L_{n+1}^N and H_{n+1}^N in a similar manner which is used for F_{n+1}^N.

5 Convergence and stability

As we are aware, the first and most important step in numerical analysis is to prove the stability and convergence of the proposed numerical method. To do so, we need to introduce some mathematical preliminaries.

Definition 5.1 [8] Suppose $\Omega = (a, b)^d$, $d \in \mathbb{N}$ and $L_{w^{\alpha,\beta}}^2(\Omega)$ is the space of square integrable functions in Ω. Now, we can define the following inner product on $L_{w^{\alpha,\beta}}^2(\Omega)$

$$(u, v)_{w^{\alpha,\beta}, \Omega} = \int_{\Omega} w^{\alpha,\beta}(X)u(X)v(X)dX, \quad \forall u, v \in L_{w^{\alpha,\beta}(\Omega)}^2,$$

$$\|u\|_{w^{\alpha,\beta}, \Omega} = \left(\int_{\Omega} w^{\alpha,\beta}(X)(u(X))^2 dX \right)^{\frac{1}{2}}, \quad \forall u \in L_{w^{\alpha,\beta}(\Omega)}^2.$$

Definition 5.2 [8] Suppose $\mathbb{P}_N^d$ is the space of all d dimensional algebraic polynomials of degree at most N in each variable. $\Pi_{N,w^{\alpha,\beta}} : L_{w^{\alpha,\beta}}^2(\Omega) \longrightarrow \mathbb{P}_N^d$ is an orthogonal projection if and only if for any $u \in L_{w^{\alpha,\beta}(\Omega)}^2$, we have

$$\int_{\Omega} (\Pi_{N,w^{\alpha,\beta}}u(X) - u(X))v(X)w^{\alpha,\beta}(X)dX = 0, \quad \forall v \in \mathbb{P}_N^d.$$

Theorem 5.1 [43] Let $\alpha, \beta > -1$. For any $u \in B_{\alpha,\beta}^m(I)$,

$$\|\Pi_N^{\alpha,\alpha}u - u\|_{l,w^{\alpha,\alpha}} \leq N^{2l-m-1/2}\|\partial_x^m u\|_{\alpha+m,\alpha+m}.$$

5.1 Convergence

In this section, we want to prove the convergence of the above method under the title of Convergence Theorem. For this purpose, using the principle of mathematical induction, we need to show that for $k = 0, 1, \ldots, M$, (for an arbitrary M) there exist positive constants L^*, H^*, F^* and R^* such that

$$|L_k^{ap} - L_k| < L^*, \quad |H_k^{ap} - H_k| < H^*, \quad |F_k^{ap} - F_k| < F^*, \quad |R_k^{ap} - R_k| < R^*, \tag{42}$$

where L_k, H_k, F_k and R_k are the exact solutions of (32)-(36) in $t = t_k$, respectively. First, we assume that

$$|L_k^{ap} - L_k| < L^*, \quad |H_k^{ap} - H_k| < H^*, \quad |F_k^{ap} - F_k| < F^*, \quad |R_k^{ap} - R_k| < R^* \quad 1 \leq k \leq n < M. \tag{43}$$

In the following, to prove the convergence theorem, we need to present the following lemma.

Lemma 5.1 *Let F be the exact solution of (21) on $[0,1] \times [0,T]$, $F_{n+1}^{ap} = F_{n+1}^N$, $\forall n \geq 1$ and $\frac{\partial^2 F}{\partial \rho^2}$ be C^1-smooth function. Then, for each $0 < \rho < 1$, there exist positive constants c_1, c_2 and c such that*

$$(\frac{1}{2} - c_1 h^*)\|\frac{\partial(F_{n+1}^N - F_{n+1})}{\partial \rho}\|_{w^{0,0}}^2 \leq \frac{1}{2}\|\frac{\partial(F_n^{ap} - F_n)}{\partial \rho}\|_{w^{0,0}}^2 +$$

$$\sum_{i=0}^{n} h^* c_2 \left(\|L_i - L_i^{ap}\|_{w^{0,0}}^2 + \|H_i - H_i^{ap}\|_{w^{0,0}}^2 + \|F_i - F_i^{ap}\|_{w^{0,0}}^2\right) + \|E_F^*\|_\infty^2 + h^* K_1(N),$$

where $K(N)$ is the error generated by the spectral method and

$$\|E_F^*\|_\infty \leq c(h^*)^2, \quad \lim_{N \to \infty} K_1(N) = 0. \tag{44}$$

Proof For every $N \in \mathbb{N}$, there exists a polynomial F_1^N such that

$$I_N^{0,0} F_1^N = F_1^N, \quad \frac{\partial F_1^N}{\partial \rho}(0,t) = 0, \quad \frac{\partial F_1^N}{\partial \rho}(1,t) = 0, \quad F_1^N(\rho, 0) = 0, \quad 0 \leq t \leq T,$$

and

$$\lim_{N \to \infty} \left(\|\frac{\partial(F_1^N - F)}{\partial \rho}\|_{\omega^{0,0}}^2 + \|F_1^N - F\|_{\omega^{0,0}}^2 + \|\frac{G(\rho)\partial(F - F_1^N)}{\partial \rho}\|_{\omega^{0,0}}^2 + \|\frac{\partial^2(F - F_1^N)}{\partial \rho^2}\|_{\omega^{0,0}}^2\right) = 0. \tag{45}$$

Now, by taking the inner product of both sides of (39), we conclude that

$$(\Pi_N^{0,0} \mathrm{L} F_{n+1}^N - \Pi_N^{0,0} \mathrm{L} F_{n+1,1}^N, \frac{\partial^2(F_{n+1}^N - F_{n+1,1}^N)}{\partial \rho^2})_{w^{0,0}} =$$

$$(I_N^{0,0} \underbrace{(g_n^* - \mathrm{L} F_{n+1,1}^N)}_{g_n^1}, \frac{\partial^2(F_{n+1}^N - F_{n+1,1}^N)}{\partial \rho^2})_{w^{0,0}},$$

where $F_{n+1,1}^N(\rho) := F_1^N(\rho, t_{n+1})$ and for each $u \in C^2[0,1]$, $\mathtt{L}$ is defined as follows

$$\mathtt{L}u = u - \frac{h^* D}{(1 - R_{n+1})} \frac{\partial^2 u}{\partial \rho^2} + h^* G(\rho) \frac{\partial u}{\partial \rho}, \tag{46}$$

where $G(\rho)$ is defined in (41) and is a bounded continuous function. Therefore we have

$$\left(F_{n+1}^N - F_{n+1,1}^N, \frac{\partial^2 (F_{n+1}^N - F_{n+1,1}^N)}{\partial \rho^2} \right)_{w^{0,0}} -$$

$$\left(\frac{h^* D}{(1 - R_{n+1}^{ap})^2} \frac{\partial^2 \left(F_{n+1}^N - F_{n+1,1}^N \right)}{\partial \rho^2}, \frac{\partial^2 (F_{n+1}^N - F_{n+1,1}^N)}{\partial \rho^2} \right)_{w^{0,0}} +$$

$$\left(h^* G(\rho) \frac{\partial (F_{n+1}^N - F_{n+1,1}^N)}{\partial \rho}, \frac{\partial^2 (F_{n+1}^N - F_{n+1,1}^N)}{\partial \rho^2} \right)_{w^{0,0}}$$
$$= (I_N^{0,0} g_n^1, \frac{\partial^2 (F_{n+1}^N - F_{n+1,1}^N)}{\partial \rho^2})_{w^{0,0}}. \tag{47}$$

Then, by using Cauchy-Schwarz inequality there exists a constant c_5 such that

$$\|\frac{\partial (F_{n+1}^N - F_{n+1,1}^N)}{\partial \rho}\|_{w^{0,0}}^2 + \frac{D h^*}{(1 - R_{n+1})^2} \|\frac{\partial^2 (F_{n+1}^N - F_{n+1,1}^N)}{\partial \rho^2}\|_{w^{0,0}}^2 \leq$$
$$c_5 h^* \|\frac{\partial (F_{n+1}^N - F_{n+1,1}^N)}{\partial \rho}\|_{w^{0,0}}^2 + |(I_N^{0,0} g_n^1, \frac{\partial^2 (F_{n+1}^N - F_{n+1,1}^N)}{\partial \rho^2})_{w^{0,0}}|. \tag{48}$$

By combining (40) with (48) we obtain that

$$\left| (I_N^{0,0} g_n^1, \frac{\partial (F_{n+1}^N - F_{n+1,1}^N)}{\partial \rho})_{w^{0,0}} \right| \leq \left| (I_N^{0,0}(g_n^* - \mathtt{L}F_{n+1,1}^N), \frac{\partial (F_{n+1}^N - F_{n+1,1}^N)}{\partial \rho})_{w^{0,0}} \right| \leq$$
$$\left| (F_n^{ap} - F_{n,1}^N - \frac{F_{n-1}^{ap} - F_{n-1,1}^N - F_n^{ap} + F_{n,1}^N}{3}, \frac{\partial^2 (F_{n+1}^N - F_{n+1,1}^N)}{\partial \rho^2})_{w^{0,0}} \right| +$$
$$\left| (I_N^{0,0}(\mathtt{L}F_{n+1,1}^N - F_{n,1}^N + \underbrace{\frac{F_{n-1,1}^N - F_{n,1}^N}{3}) - I_N^{0,0} f_n^*}_{g_n^2}, \frac{\partial^2 (F_{n+1}^N - F_{n+1,1}^N)}{\partial \rho^2})_{w^{0,0}} \right|. \tag{49}$$

Therefore, from (48) and (49) and using Cauchy-Schwarz inequality and Young inequality, we get that

$$\|\frac{\partial (F_{n+1}^N - F_{n+1,1}^N)}{\partial \rho}\|_{w^{0,0}}^2 + \frac{D h^*}{(1 - R_{n+1})^2} \|\frac{\partial^2 (F_{n+1}^N - F_{n+1,1}^N)}{\partial \rho^2}\|_{w^{0,0}}^2 \leq$$

$$(g_n^2, \frac{\partial^2 (F_{n+1}^N - F_{n+1,1}^N)}{\partial \rho^2})_{w^{0,0}} + c_5 h^* \|\frac{\partial (F_{n+1}^N - F_{n+1,1}^N)}{\partial \rho}\|_{w^{0,0}}^2 + \frac{1}{2} \|\frac{\partial (F_n^{ap} - F_{n,1}^N)}{\partial \rho}\|_{w^{0,0}}^2 +$$

$$\frac{1}{2} \|\frac{\partial (F_{n+1}^N - F_{n+1,1}^N)}{\partial \rho}\|_{w^{0,0}}^2 + \frac{1}{3} \left| (\frac{\partial (F_{n-1}^{ap} - F_{n-1,1}^N - F_n^{ap} + F_{n,1}^N)}{\partial \rho}, \frac{\partial (F_{n+1}^N - F_{n+1,1}^N)}{\partial \rho})_{w^{0,0}} \right|.$$

So there exists a positive constant c_4 such that

$$\frac{1}{2}\|\frac{\partial(F_{n+1}^N - F_{n+1,1}^N)}{\partial\rho}\|_{w^{0,0}}^2 + \frac{Dh^*}{2(1-R_{n+1})^2}\|\frac{\partial^2(F_{n+1}^N - F_{n+1,1}^N)}{\partial\rho^2}\|_{w^{0,0}}^2 \le$$

$$+h^*c_4\|2f_n^F - f_{n-1}^F + E^F - 2f_n^{F,ap} + f_{n-1}^{F,ap}\|_{w^{0,0}}^2 + |(L_nF_{n,1}^N - L_nF, \frac{\partial^2(F_{n+1}^N - F_{n+1,1}^N)}{\partial\rho^2})_{w^{0,0}}|+$$

$$c_5h^*\|\frac{\partial(F_{n+1}^N - F_{n+1,1}^N)}{\partial\rho}\|_{w^{0,0}}^2 + \frac{1}{2}\|\frac{\partial(F_n^{ap} - F_{n,1}^N)}{\partial\rho}\|_{w^{0,0}}^2+$$

$$\frac{1}{3}\left|(\frac{\partial(F_{n-1}^{ap} - F_{n-1,1}^N - F_n^{ap} + F_{n,1}^N)}{\partial\rho}, \frac{\partial(F_{n+1}^N - F_{n+1,1}^N)}{\partial\rho})_{w^{0,0}}\right|, \tag{50}$$

where

$$L_nu = Lu_{n+1} - u_n + \frac{u_{n-1} - u_n}{3}, \tag{51}$$

and L is defined in (46). On the other hand, from (39) we have

$$\left|(\frac{\partial(F_n^{ap} - F_{n,1}^N - F_{n+1}^{ap} + F_{n+1,1}^N)}{\partial\rho}, \frac{\partial(F_{n+1}^N - F_{n+1,1}^N)}{\partial\rho})_{w^{0,0}}\right| + \frac{h^*D}{2(1-R_{n+1})^2}\|\frac{\partial^2(F_{n+1}^N - F_{n+1,1}^N)}{\partial\rho^2}\|_{w^{0,0}}^2 \le$$

$$h^*c_4\|\frac{\partial(F_{n+1}^N - F_{n+1,1}^N)}{\partial\rho}\|_{w^{0,0}}^2 + h^*M_4^F\|2f_n^F - f_{n-1}^F + E^F - 2f_n^{F,ap} + f_{n-1}^{F,ap}\|_{w^{0,0}}^2+$$

$$\frac{1}{3}\left|(\frac{\partial(F_n^{ap} - F_{n,1}^N - F_{n+1}^{ap} + F_{n+1,1}^N)}{\partial\rho}, \frac{\partial(F_{n+1}^N - F_{n+1,1}^N)}{\partial\rho})_{w^{0,0}}\right|+$$

$$|(L_nF_{n,1}^N - L_nF, \frac{\partial^2(F_{n+1}^N - F_{n+1,1}^N)}{\partial\rho^2})_{w^{0,0}}|, \tag{52}$$

where

$$f_i^{j,ap} = f^j(L_i^{ap}, H_i^{ap}, F_i^{ap}), \quad f_i^j = f^j(L_i, H_i, F_i), \quad j \in \{L, H, F\}.$$

Then, by applying the recurrence relation (52) repeatedly in (50) we can conclude that

$$(\frac{1}{2} - c_1h^*)\|\frac{\partial(F_{n+1}^N - F_{n+1,1}^N)}{\partial\rho}\|_{w^{0,0}}^2 \le \frac{1}{2}\|\frac{\partial(F_n^{ap} - F_{n,1}^N)}{\partial\rho}\|_{w^{0,0}}^2+$$

$$\sum_{i=0}^n \frac{1}{3^i}h^*c_2 \left(\|L_{i,1}^N - L_i^{ap}\|_{w^{0,0}}^2 + \|H_{i,1}^N - H_i^{ap}\|_{w^{0,0}}^2 + \|F_{i,1}^N - F_i^{ap}\|_{w^{0,0}}^2\right)+$$

$$h^*\|E_F^*\|_\infty^2 + h^*K_1(N). \tag{53}$$

where $\|E_F^*\|_\infty$ and $K_1(N)$ are as in (44).

∎

Lemma 5.2 Let $F_{n+1}^{ap} = F_{n+1}^N$, $\forall n \ge 1$ and $\frac{\partial^2 F}{\partial\rho^2}$ be C^1-smooth function. Then, for each $0 < \rho < 1$, there exist positive constants M^* and C^* such that the following inequality holds

$$(F_{n+1}^N - F_{n+1,1}^N)^2\Big|_{\rho=1} \le F^*+ \tag{54}$$

$$4(\frac{1}{3})^{n-1}\left(\frac{h^*D}{2(1-R_{n+1})^2} + \frac{C^*}{\sqrt{N}}\right)(L^{*2} + H^{*2} + F^{*2} + h^*\|E_F^*\|_\infty^2 + h^*K_1(N)) \le M^*.$$

where L^*, H^* and F^* are obtained from (42) and $\|E_F^*\|_\infty$ and $K_1(N)$ are as in (44).

Proof By taking the inner product of both sides of (39), we can deduce that

$$(\Pi_N^{0,0}\mathsf{L}F_{n+1}^N - \Pi_N^{0,0}\mathsf{L}F_{n+1,1}^N, \rho\frac{\partial}{\partial\rho}(\rho\frac{\partial(F_{n+1}^N - F_{n+1,1}^N)}{\partial\rho})) =$$

$$(I_N^{0,0}(g_n^* - \mathsf{L}F_{n+1,1}^N), \rho\frac{\partial}{\partial\rho}(\rho\frac{\partial(F_{n+1}^N - F_{n+1,1}^N)}{\partial\rho})).$$

Using (53), (42), Theorem 5.1, Definition 5.2, Cauchy-Schwarz inequality and Young inequality, we have

$$\left.(F_{n+1}^N - F_{n+1,1}^N)^2\right|_{\rho=1} \le F^* +$$

$$4(\frac{1}{3})^{n-1}\left(\frac{h^* D}{2(1 - R_{n+1})^2} + \frac{\max\{1, c_5\}}{\sqrt{N}}\right)(L^{*2} + H^{*2} + F^{*2} + h^*\|E_F^*\|_\infty^2 + h^* K_1(N)) \le M^*, \quad (55)$$

where c_5 is obtained from (48). ∎

Finally, using Lemmas 5.1 and 5.2 we have

$$(\frac{1}{2} - c_1 h^*)\|\frac{\partial(F_{n+1}^N - F_{n+1,1}^N)}{\partial\rho}\|_{w^{0,0}}^2 \le \frac{1}{2}\|\frac{\partial(F_n^{ap} - F_{n,1}^N)}{\partial\rho}\|_{w^{0,0}}^2 +$$

$$\sum_{i=0}^n \frac{1}{3^i} h^* c_2 \left(\|\frac{\partial(L_{i,1}^N - L_i^{ap})}{\partial\rho}\|_{w^{0,0}}^2 + \|\frac{\partial(H_{i,1}^N - H_i^{ap})}{\partial\rho}\|_{w^{0,0}}^2 + \|\frac{\partial(F_{i,1}^N - F_i^{ap})}{\partial\rho}\|_{w^{0,0}}^2\right) +$$

$$h^*\|E_F^*\|_\infty^2 + h^* K_1(N), \quad (56)$$

where $\|E_F^*\|_\infty$ and $K_1(N)$ are as in (44).

Similar to the proof of lemma 5.1, we can show that there exist positive constants c_6, c_7, c_8, c_9 such that for $0 \le t \le T$,

$$(\frac{1}{2} - c_6 h^*)\|\frac{\partial(L_{n+1}^N - L_{n+1,1}^N)}{\partial\rho}\|_{w^{0,0}}^2 \le \frac{1}{2}\|\frac{\partial(L_n^{ap} - L_{n,1}^N)}{\partial\rho}\|_{w^{0,0}}^2 +$$

$$\sum_{i=0}^n \frac{1}{3^i} h^* c_7 \left(\|\frac{\partial(L_{i,1}^N - L_i^{ap})}{\partial\rho}\|_{w^{0,0}}^2 + \|\frac{\partial(F_{i,1}^N - F_i^{ap})}{\partial\rho}\|_{w^{0,0}}^2\right) + h^*\|E_L^*\|_\infty^2 + h^* K_2(N), \quad (57)$$

$$(\frac{1}{2} - c_8 h^*)\|\frac{\partial(H_{n+1}^N - H_{n+1,1}^N)}{\partial\rho}\|_{w^{0,0}}^2 \le \frac{1}{2}\|\frac{\partial(H_n^{ap} - H_{n,1}^N)}{\partial\rho}\|_{w^{0,0}}^2 +$$

$$\sum_{i=0}^n \frac{1}{3^i} h^* c_9 \left(\|\frac{\partial(H_{i,1}^N - H_i^{ap})}{\partial\rho}\|_{w^{0,0}}^2 + \|\frac{\partial(F_{i,1}^N - F_i^{ap})}{\partial\rho}\|_{w^{0,0}}^2\right) + h^*\|E_H^*\|_\infty^2 + h^* K_3(N), \quad (58)$$

where

$$\lim_{N\to\infty} K_2(N) = 0, \ \lim_{N\to\infty} K_3(N) = 0 \quad \text{and} \quad \max\{\|E_L^*\|_\infty, \|E_H^*\|_\infty\} < c(h^*)^2,$$

and c is a positive constant.

In the following theorem, the convergence of the proposed method is proved.

Theorem 5.2 *(Convergence Theorem) Let $L_{n+1}^{ap} = L_{n+1}^N$, $H_{n+1}^{ap} = H_{n+1}^N$ and $F_{n+1}^{ap} = F_{n+1}^N$. Under the assumption of Lemma 5.1 there exist positive constants M_1, M_2 such that*

$$\max_{k=0,\ldots,n+1}\{\xi_k\} \le M_1(e^{M_2 T})(h^{*2} + (K(N))^{\frac{1}{2}}),$$

where

$$\xi_k = \|\frac{\partial(L_k^{ap} - L_k)}{\partial\rho}\|_{w^{0,0}} + \|\frac{\partial(H_k^{ap} - H_k)}{\partial\rho}\|_{w^{0,0}} + \|\frac{\partial(F_k^{ap} - F_k)}{\partial\rho}\|_{w^{0,0}} + |R_k^{ap} - R_k|,$$

$$\lim_{N\to\infty} K(N) = 0.$$

Proof From (56), (57) and (58) we can conclude that there exists a constant M_4, such that

$$\max_{k=0,\ldots,n+1}\{\phi_k\} \le (1+M_4 h^*)\phi_n + (1+M_4 h^*)^2 \max\{\phi_k\}_{k=0,1,\ldots n} + (1+M_4 h^*)(h^*\|E_F^*\|_\infty^2 + h^* K(N)),$$

where

$$\phi_k = \|\frac{\partial(L_k^{ap} - L_k)}{\partial\rho}\|_{w^{0,0}}^2 + \|\frac{\partial(H_k^{ap} - H_k)}{\partial\rho}\|_{w^{0,0}}^2 + \|\frac{\partial(F_k^{ap} - F_k)}{\partial\rho}\|_{w^{0,0}}^2 + |R_k^{ap} - R_k|^2,$$

$$\lim_{N\to\infty} K(N) = 0.$$

and $\|E_F^*\|$ is as in (44). Therefore, there exists a constant M_3 that

$$\max_{k=0,\ldots,n+1}\{\phi_k\} \le (1+M_3 h^*)\max\{\phi_k\}_{k=0,1,\ldots n} + (1+M_3 h^*)(h^*\|E_F^*\|_\infty^2 + h^* K(N)).$$

Then, by applying the above recurrence relation we have

$$\max_{k=0,\ldots,n+1}\{\phi_k\} \le (1+M_3 h^*)^{n+1}\phi_0 + |\frac{(1+M_3 h^*)^{n+1} - 1}{M_3 h^*}|(h^*\|E_F^*\|_\infty^2 + h^* K(N)).$$

Finally, it may be concluded that there exist constants M_1 and M_2 such that

$$\max_{k=0,\ldots,n+1}\{\xi_k\} \le M_1(e^{M_2 T})(h^{*2} + (K(N))^{\frac{1}{2}}). \tag{59}$$

■

Employing the General Sobolev inequalities, there exists a positive constant M_5 such that for $0 \le t \le T$,

$$|F_{n+1}^{ap} - F_{n+1}| \le M_5\|F_{n+1}^{ap} - F_{n+1}\|_{w^{0,0}}. \tag{60}$$

Using (60) and (56), we can choose proper N and h such that

$$|F_{n+1}^{ap} - F_{n+1}| \leq F^*. \tag{61}$$

Similar to the proof of the Theorem 5.2 and (61), we can show that

$$|L_{n+1}^{ap} - L_{n+1}| \leq L^*, \tag{62}$$

and

$$|H_{n+1}^{ap} - H_{n+1}| \leq H^*. \tag{63}$$

Thus, using (61), (62), (63) and Theorem 5.2, we can deduce that the sequence $\{L_n, H_n, F_n, R_n\}_{n=0}^{\infty}$ converges to the exact solution of the problem (6)-(10) on $[0,1] \times [0,T]$. Now, using the principle of mathematical induction, Theorem (5.2), (42), (43), (61), (62) and (63), we have

$$|L_k^{ap} - L_k| < L^*, \quad |H_k^{ap} - H_k| < H^*, \quad |F_k^{ap} - F_k| < F^*, \quad |R_k^{ap} - R_k| < R^*, \quad 0 \leq k \leq M. \tag{64}$$

5.2 Stability

In this section, we want to prove the stability of the presented method. For this purpose, first, we consider the perturbed problem as follows

$$\frac{\partial L}{\partial t} - \frac{1}{(1-R(t))^2} \frac{\partial^2 L}{\partial \rho^2} +$$
$$\left(\frac{-2}{\rho(1-R(t))^2 + R(t)(1-R(t))} + \frac{v(0,t)(\rho-1)}{1-R(t)} + \frac{2(1-\rho)\alpha}{1-R(t)} \right) \frac{\partial L}{\partial \rho} = f^L(L,F) + p_1(\rho,t),$$
$$\frac{\partial L}{\partial \rho} = 0 \text{ at } \rho = 0,\ t > 0, \quad \frac{\partial L}{\partial \rho} = 0 \text{ at } \rho = 1,\ t > 0, \quad L(\rho,0) = 0, \tag{65}$$

$$\frac{\partial H}{\partial t} - \frac{1}{(1-R(t))^2} \frac{\partial^2 H}{\partial \rho^2} +$$
$$\left(\frac{-2}{\rho(1-R(t))^2 + R(t)(1-R(t))} + \frac{v(0,t)(\rho-1)}{1-R(t)} + \frac{2(1-\rho)\alpha}{1-R(t)} \right) \frac{\partial H}{\partial \rho} = f^H(H,F) + p_2(\rho,t),$$
$$\frac{\partial H}{\partial \rho} = 0 \text{ at } \rho = 0,\ t > 0, \quad \frac{\partial H}{\partial \rho} = 0 \text{ at } \rho = 1,\ t > 0, \quad H(\rho,0) = 0, \tag{66}$$

$$\frac{\partial F}{\partial t} - \frac{D}{(1-R(t))^2} \frac{\partial^2 F}{\partial \rho^2} +$$
$$\left(\frac{-2D}{\rho(1-R(t))^2 + R(t)(1-R(t))} + \frac{v}{1-R(t)} + \frac{v(0,t)(\rho-1)}{1-R(t)} + \frac{2D(1-\rho)\beta}{1-R(t)} \right) \frac{\partial F}{\partial \rho}$$
$$= f^F(L,H,F) + p_3(\rho,t), \tag{67}$$

$$\frac{\partial F}{\partial \rho} = 0 \text{ at } \rho = 0,\ t > 0, \quad \frac{\partial F}{\partial \rho} = 0 \text{ at } \rho = 1,\ t > 0, \quad F(\rho,0) = 0, \tag{68}$$

$$\frac{1}{1 - R(t)}\frac{\partial v}{\partial \rho} = f^v(L, H, F) + p_4(\rho, t),$$

$$v(\rho, t) = 0 \text{ at } \rho = 1, \ t > 0, \tag{69}$$

$$\frac{dR}{dt} = v(0, t), \ t > 0,$$

$$R(0) = \epsilon. \tag{70}$$

In the following theorem, the stability of the proposed method is proved.

Theorem 5.3 *Let ϵ_1 be a positive constant and $|p_i| < \epsilon_1$ $(i = 1, \ldots, 4)$. Then, under the assumptions of Lemma 5.1, there exist positive constants M_1^*, M_2^* such that*

$$\max_{k=0,\ldots,n+1}\{\xi_k\} \le M_1^*(e^{M_2^*T} - 1)(h^{*2} + \epsilon_1 + (K(N))^{\frac{1}{2}}),$$

where

$$\xi_k = \|\frac{\partial(L_k^{ap} - L_k)}{\partial \rho}\|_{w^{0,0}} + \|\frac{\partial(H_k^{ap} - H_k)}{\partial \rho}\|_{w^{0,0}} + \|\frac{\partial(F_k^{ap} - F_k)}{\partial \rho}\|_{w^{0,0}} + |R_k^{ap} - R_k|.$$

Proof If we solve the perturbed problem (65)-(70) using the presented method, one can conclude that there exist a positive constant M_4^* such that

$$\max_{k=0,\ldots,n+1}\{\phi_k\} \le (1+M_4^*h^*)\phi_n + (1+M_4^*h^*)^2 \max\{\phi_k\}_{k=0,1,\ldots n} + (1+M_4^*h^*)(h^*\|E\|_\infty^2 + h^*K(N) + h^*\epsilon_1),$$

where $\|E\|_\infty \le M^*h^{*2}$ and M^* is a positive constant and also,

$$\phi_k = \|\frac{\partial(L_k^{ap} - L_k)}{\partial \rho}\|_{w^{0,0}}^2 + \|\frac{\partial(H_k^{ap} - H_k)}{\partial \rho}\|_{w^{0,0}}^2 + \|\frac{\partial(F_k^{ap} - F_k)}{\partial \rho}\|_{w^{0,0}}^2 + |R_k^{ap} - R_k|^2,$$

$$\lim_{N\to\infty} K(N) = 0.$$

So we get

$$\max_{k=0,\ldots,n+1}\{\phi_k\} \le (1 + M_3^*h^*) \max\{\phi_k\}_{k=0,1,\ldots n} + (1 + M_3^*h^*)(h^*\|E\|_\infty^2 + h^*K(N) + h^*\epsilon_1),$$

then, by applying the above recurrence relation we have

$$\max_{k=0,\ldots,n+1}\{\phi_k\} \le (1 + M_3^*h^*)^{n+1}\phi_0 + |\frac{(1 + M_3^*h^*)^{n+1} - 1}{M_3^*h^*}|(h^*\|E\|_\infty^2 + h^*K(N) + h^*\epsilon_1).$$

Therefore, there exist costats M_1^* and M_2^* such that we have

$$\max_{k=0,\ldots,n+1}\{\xi_k\} \le M_1^*(e^{M_2^*T})(h^{*2} + \epsilon_1 + (K(N))^{\frac{1}{2}}).$$

∎

6 Numerical experiments

The main target of this section is to investigate the numerical solution of the model of Atherosclerosis from two perspectives: 1-numerical solution point of view 2-biological simulation point of view. We first examine the numerical results from the first perspective. We solve the model of Atherosclerosis by applying the finite difference/collocation method. The most important question to ask is how to construct trial functions which satisfy the boundary condition to establish the collocation method. The first and simple way that comes to mind is to use a linear combination of monomial polynomials. So, we approximate the functions $L(\rho, t), H(\rho, t), F(\rho, t)$ in the form of (37) as follows

$$L_{n+1}^N(\rho) = \sum_{i=0}^{N} l_i^{n+1} p_i(\rho), \quad H_{n+1}^N(\rho) = \sum_{i=0}^{N} h_i^{n+1} p_i(\rho), \quad F_{n+1}^N(\rho) = \sum_{i=0}^{N} f_i^{n+1} p_i(\rho),$$

where

$$p_i(\rho) = \frac{\rho^{i+2}}{i+2} - \frac{\rho^{i+1}}{i+1}, \quad i = 1, 2, \ldots, N,$$

which will denote by "TFBM" (Trial Functions Based on Monomials). Also, the Gauss quadrature points $\{x_i^{0,0}\}_{i=1}^N$ (i.e., the zeros of Legendre polynomial of degree $N+1$) are considered as collocation points. The typical parameter values and the initial conditions for our numerical simulations are: $k_1 = 10$, $k_2 = 10$, $K_1 = 10^{-2}$, $K_2 = 0.5$, $D = 8.64 \times 10^{-7}$, $\mu_1 = 0.015$, $\mu_2 = 0.03$, $r_1 = 2.42 \times 10^{-5}$, $r_2 = 5.45 \times 10^{-7}$, $\lambda = 2.573 \times 10^{-3}$, $\delta = -2.541 \times 10^{-3}$, $M_0 = 5 \times 10^{-5}$, $\alpha = 1$, $\beta = 0.01$, $L_0 = 14 \times 10^{-4}$, $H_0 = 6 \times 10^{-4}$, $F_0 = 0$, which are taken from [19, 22]. Notice that in our simulations, the radius of initial plaque ϵ in (5) is considered to be 0.9 cm.

Now, in order to verify our numerical results, we need to present the following definition.

Definition 6.1 A sequence $\{x_n\}_{n=1}^{\infty}$ is said to converge to x with order p if there exists a constant C such that $|x_n - x| \leq C n^{-p}, \quad \forall n$. This can be written as $|x_n - x| = \mathcal{O}(n^{-p})$. A practical method to calculate the rate of convergence for a discretization method is to use the following formula

$$p \approx \frac{\log_e(e_{n_2}/e_{n_1})}{\log_e(n_1/n_2)}, \tag{71}$$

where e_{n_1} and e_{n_2} denote the errors with respect to the step sizes $\frac{1}{n_1}$ and $\frac{1}{n_2}$, respectively [20].

It is valuable to point out that our numerical calculations are carried out using the **MATLAB 2018a** program in a computer with the Intel Core i7 processor (2.90 GHz, 4 physical cores).

Error of	M=100	M=200	M=300	M=400	M=500	M=600
L	$1.832329e-05$	$7.33126e-06$	$4.11065e-06$	$2.58829e-06$	$1.70362e-06$	$1.12596e-06$
H	$2.57909e-07$	$1.03322e-07$	$5.79623e-08$	$3.65061e-08$	$2.40324e-08$	$1.58853e-08$
F	$6.60404e-09$	$4.21233e-09$	$3.16373e-09$	$2.26606e-09$	$1.60468e-09$	$1.11186e-09$

Table 1: *Maximum time-error with N=10 and various M by considering TFBM.*
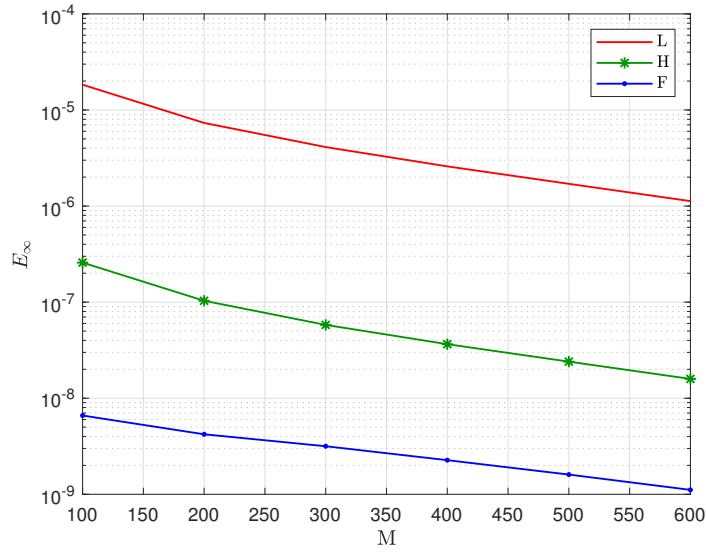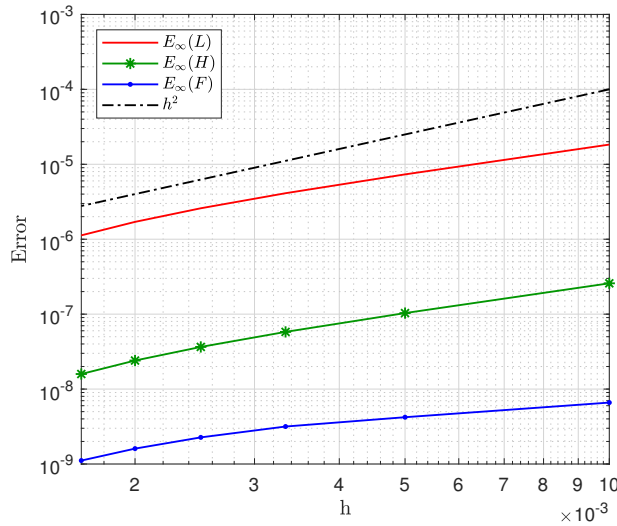

Fig. 3: *Maximum time-error functions with N=10 and various M by considering TFBM.*

Lies in the fact that it is hard or sometimes impossible to reach the exact solution of most of the coupled nonlinear models analytically, and because we have shown that the presented method for solving the model is stable and convergent (See Theorem 5.2), so, we consider numerical results for the large $M = 300$ and $N = 10$ as an exact solution and for other values of M, we report the time-error in Table 1. To better see the time-error of the presented approach numerically, we report the obtained results in Figure 3. As we see in Table 2 and Figure 4, the non-classical finite difference method presented in (24) has almost $\mathcal{O}(h^2)$ error, which verifies our theoretical results presented in Theorem 5.2.

Error	N=2	N=4	N=6	N=8
L	0.399186e-05	0.286885e-05	0.190745e-05	0.119180e-05
H	0.504070e-06	0.359887-06	0.239578e-06	0.149847e-06
F	0.293787e-07	0.217007e-07	0.144762e-07	0.905871e-08

Table 3: *Maximum space-error with M=100 and various N by considering TFBM.*

CN	N=4	N=6	N=8	N=10	N=12	N=14	N=16	N=18	N=20
Eq. (1)	272e+04	115e+06	529e+07	258e+09	131e+11	689e+12	**369e+12**	**202e+15**	**singular**
Eq. (2)	272e+04	115e+06	529e+07	258e+09	131e+11	689e+12	**369e+12**	**202e+15**	**singular**
Eq. (3)	367e+05	303e+07	229e+09	166e+11	117e+13	814e+14	**558e+15**	**380e+17**	**singular**

Table 4: *Condition number of the coefficient matrices (CN).*

	Rate of convergence for		
M	L	H	F
100	-	-	-
200	1.321	1.319	0.648
300	1.426	1.425	0.706
400	1.607	1.607	1.159
500	1.874	1.873	1.546
600	2.271	2.270	2.012

Fig. 4: *The behaviour of Maximum time-error with N=10 and various M in Log-Log scale by considering TFBM.*

Table 2: *The rate of convergence with respect to time variable with N=10 and various M by considering TFBM.*

In Table 3, we have presented the maximum space-errors with $M = 100$ and various values of N. To better see the space-error of numerical results, Figure 5 is presented. It is worth to note that in the numerical results, the discrepancy between an exact value and some approximation to it, is called "maximum error" and is denoted by E_∞. In Table 4, the condition numbers (CN) of the coefficient matrices of the collocation method are shown. In this table, high values of condition numbers are
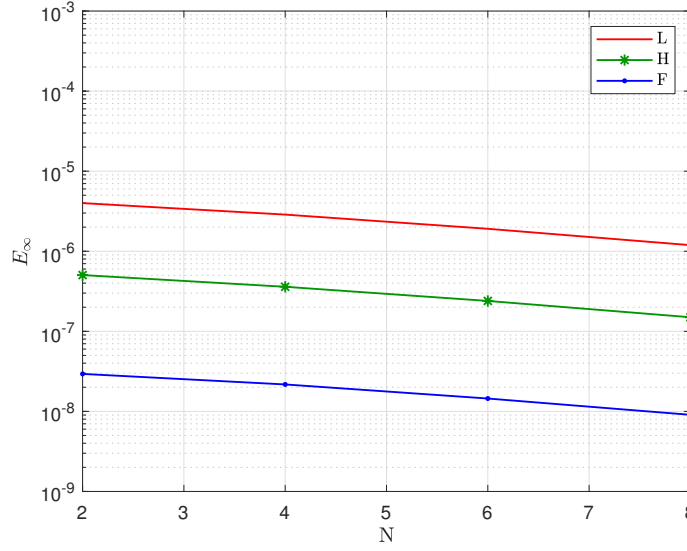
Fig. 5: *Maximum space-error functions with M=100 and various N by considering TFBM.*

highlighted in bold. Because of the fact that the condition number of the coefficient matrices grows very fast when $N > 10$, unfortunately, the Matlab software can not accurately extract the results. To overcome this difficulty, we need to propose proper trial functions which reduce the condition number significantly. In this case, we decide to consider Legendre polynomials (Jacobi polynomials with $\alpha = \beta = 0$) to construct trial functions for the collocation method [12]. So, let $L_n(x)$ be the Legendre polynomial of degree n and set

$$p_n(x) = L_n(x) + c_n L_{n+1}(x) + d_n L_{n+2}(x), \quad n \geq 0, \tag{72}$$

where the constants c_n and d_n are uniquely determined in such a way that $p_n(x)$ satisfies the boundary conditions; in other word, $\dfrac{\partial p_n}{\partial x}(\pm 1) = 0, \quad \forall n \geq 0$.

According to the features of Legendre polynomials we have

$$\frac{\partial p_n}{\partial x}(\pm 1) = \frac{\partial L_n}{\partial x}(\pm 1) + c_n \frac{\partial L_{n+1}}{\partial x}(\pm 1) + d_n \frac{\partial L_{n+2}}{\partial x}(\pm 1) =$$
$$\frac{1}{2}(\pm 1)^{n-1} n(n+1) + c_n \frac{1}{2}(\pm 1)^n (n+1)(n+2) + d_n \frac{1}{2}(\pm 1)^{n+1}(n+2)(n+3) = 0, \tag{73}$$

therefore, by solving (73) one can easily conclude that

$$c_n = 0, \quad d_n = -\frac{n(n+1)}{(n+2)(n+3)}. \tag{74}$$

Error of	M=100	M=200	M=300	M=400	M=500	M=600
L	$2.21985e-06$	$9.74874e-07$	$5.66407e-07$	$3.63391e-07$	$2.41969e-07$	$1.61184e-07$
H	$8.08703e-06$	$3.67228e-06$	$2.13760e-06$	$1.37270e-06$	$9.14550e-07$	$6.09439e-07$
F	$3.89421e-06$	$1.68696e-06$	$9.75669e-07$	$6.24533e-07$	$4.15285e-07$	$2.76382e-07$

Table 5: *Maximum time-error with N=50 and various M by considering TFBL.*
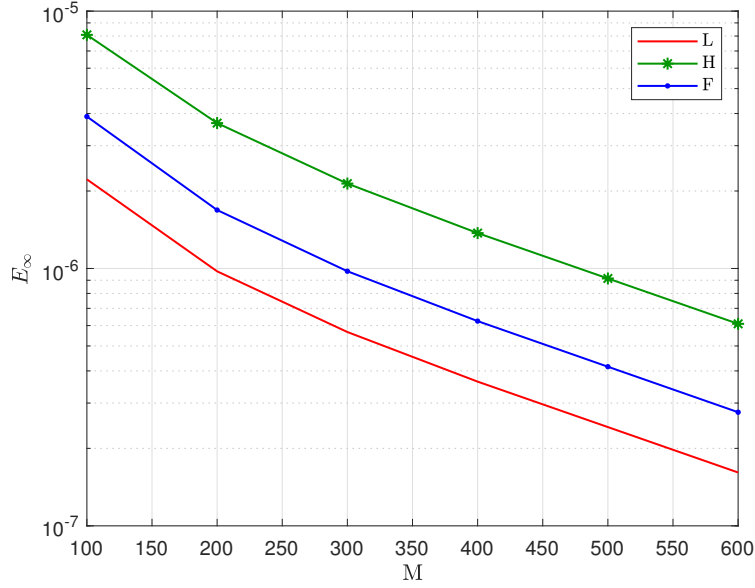

Fig. 6: *Maximum time-error with N=50 and various M by considering TFBL.*

Thus (72) becomes as follows

$$p_n(x) = L_n(x) - \frac{n(n+1)}{(n+2)(n+3)} L_{n+2}(x), \quad n \geq 0. \tag{75}$$

So we can approximate the functions $L(\rho,t), H(\rho,t), F(\rho,t)$ in the form of (37) as follows

$$L_{n+1}^N(\rho) = \sum_{i=0}^N l_i^{n+1} p_i(\rho), \quad H_{n+1}^N(\rho) = \sum_{i=0}^N h_i^{n+1} p_i(\rho), \quad F_{n+1}^N(\rho) = \sum_{i=0}^N f_i^{n+1} p_i(\rho),$$

where

$$p_i(\rho) = L_i(\rho) - \frac{(i+1)i}{(i+3)(i+2)} L_{i+2}(\rho), \quad i = 0, \ldots, N, \tag{76}$$

which we will denote by "TFBL" (Trial Functions Based on Legendre polynomials).

Remark 6.1 The scaling factors in the trial functions (76) play the role of precondition factor for the collocation matrices and reduce the condition number. [26, 29].

Error of	N=10	N=20	N=40	N=80	N=100
L	$1.53065e-10$	$7.04107e-12$	$6.98306e-13$	$1.21789e-13$	$7.34745e-14$
H	$2.96583e-11$	$8.76799e-13$	$2.18054e-13$	$8.28391e-14$	$5.54617e-14$
F	$1.44016e-11$	$6.17966e-12$	$3.09801e-12$	$1.69595e-12$	$1.34437e-12$

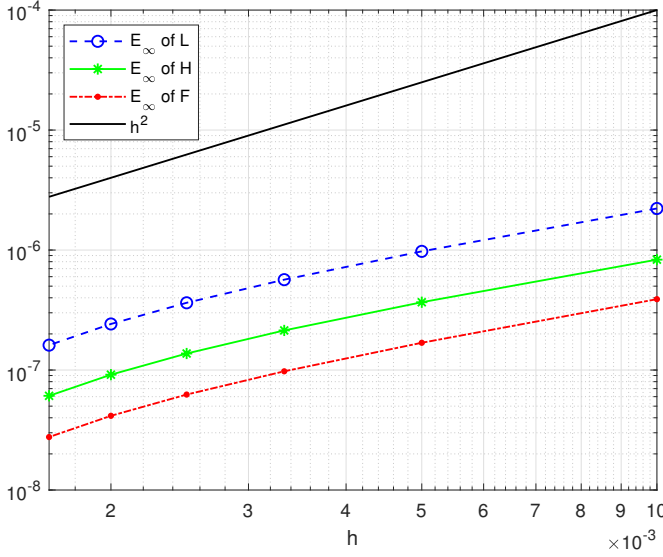**Table 7:** *Maximum space-error with M=200 and various N by considering TFBL.*

Fig. 7: *The behaviour of maximum time error with N=50 and various M in Log-Log scale by considering TFBL.*

	Rate of convergence for		
M	L	H	F
100	-	-	-
200	1.118	1.179	1.206
300	1.339	1.334	1.350
400	1.542	1.539	1.550
500	1.822	1.822	1.828
600	2.228	2.226	2.223

Table 6: *The rate of convergence with respect to the time variable with N=50 and various M by considering TFBL.*

It should be noted that in order to use Legendre polynomials, we map the domain of the problem (19)-(23) to $[-1, 1]$.

We also point out that the Gauss quadrature points $\{x_i^{0,0}\}_{i=1}^N$ are considered as the collocation points. As mentioned in TFBM case, because of the stability and convergence of the presented method, we consider the solution of the problem with $N = 100$ and $M = 1000$ as an exact solution. In Table 5, we have presented the maximum time-error $N = 51$ and various values of M. It is observed that the time-error of the presented approach numerically, we report the obtained results in Figure 6. As we can see from Table 6 and Figure 7, the non-classical finite difference method presented in (24) has almost $\mathcal{O}(h^2)$ error, which verifies our theoretical results presented in convergence Theorem 5.2. In Table 7, we illustrate the maximum space-errors $M = 200$ and various values of N by considering the solution of
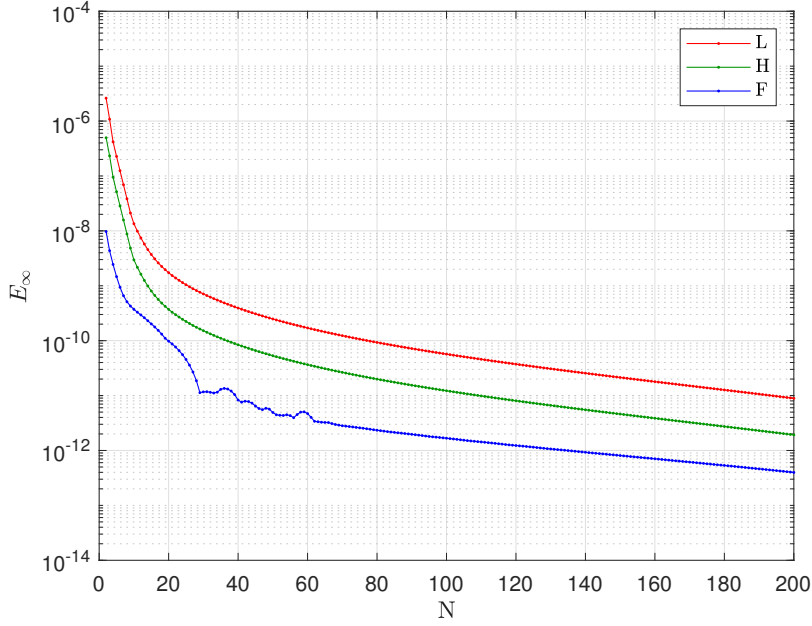
Fig. 8: *Maximum space error function for M=200 and various N.*

the problem with $N = 200$ and $M = 200$ as an exact solution. To better observe the space-error of numerical results, Figure 8 is presented. Also, the condition number of the coefficient matrices constructed by collocation method for equations (1)-(4) are shown in Table 8 and Figure 9; which shows that, as we expect from TFBL, the condition number of matrices do not increase significantly by increasing N even for $N = 150$. For a better comparison of condition numbers in both TFBM and TFBL cases, Figure 10 is presented. One can easily see that using Legendre polynomials, the condition number of the coefficient matrices in the collocation method is significantly less than TFBM.

Now, in this position, the examination of the numerical solutions from the perspective of biology and simulation is reported by presenting the rate of tumor growth with three various values of pairs (L_0, H_0). The results are presented in Table 9 and Figure 11, and they are compared to the risk map illustrated in figure 12 and Retrieved from [19]. As we expect, the level of L_0 and H_0 in blood directly affects the growth and shrink of the plaque, that means for the values of (L_0, H_0) below the "zero growth", the plaque grows as shown in Figure 13, and for the values of (L_0, H_0) above the "zero growth" the plaque shrinks, as shown in Figure 14. To better see the radius changes, a small part of the plaque in the vessel is magnified and is presented in the figures mentioned above. It is
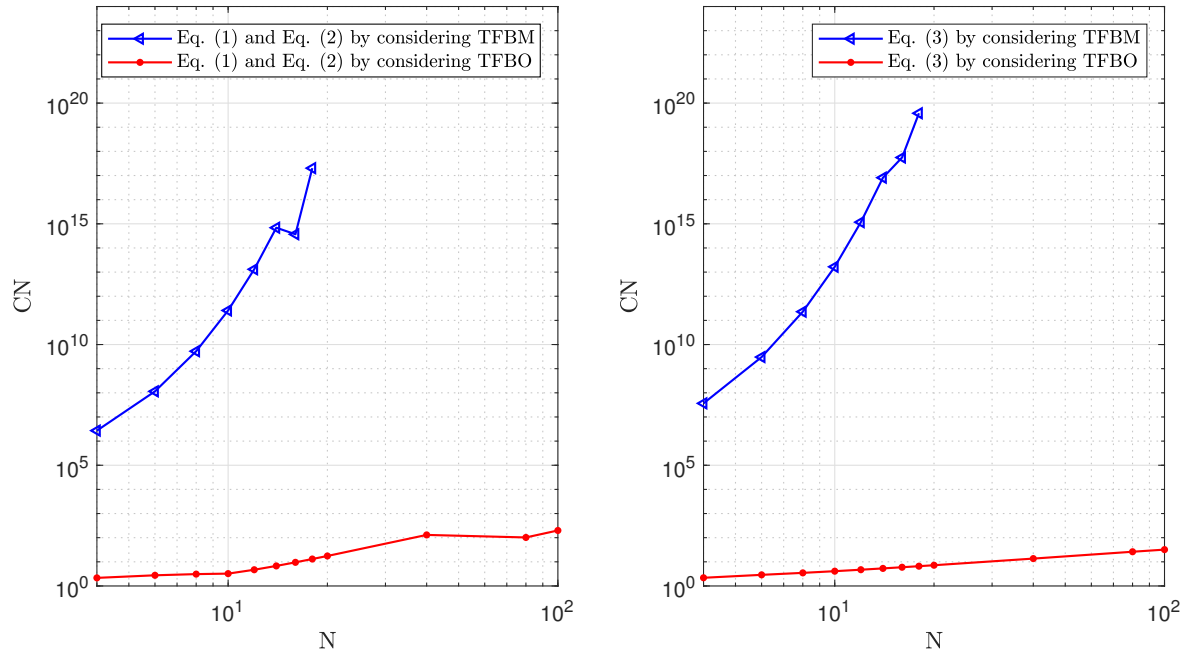
Fig. 10: *Comparison of condition numbers of the coefficient matrices in both TFBM and TFBL cases.*

noteworthy that arrows in these two figures indicate the direction of growth or shrink of the plaque.
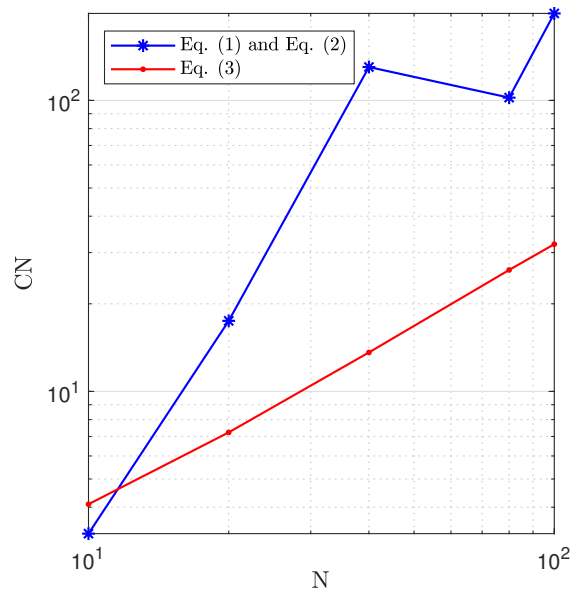

N	Eq. (1)	Eq. (2)	Eq. (3)
10	3.245	3.245	4.096
20	17.475	17.475	7.230
40	1.302e+02	1.302e+02	13.61
80	1.022e+02	1.022e+02	26.14
100	1.990e+02	1.990e+02	32.05

Fig. 9: *Condition number of the coeffi-
cient matrices (CN).*

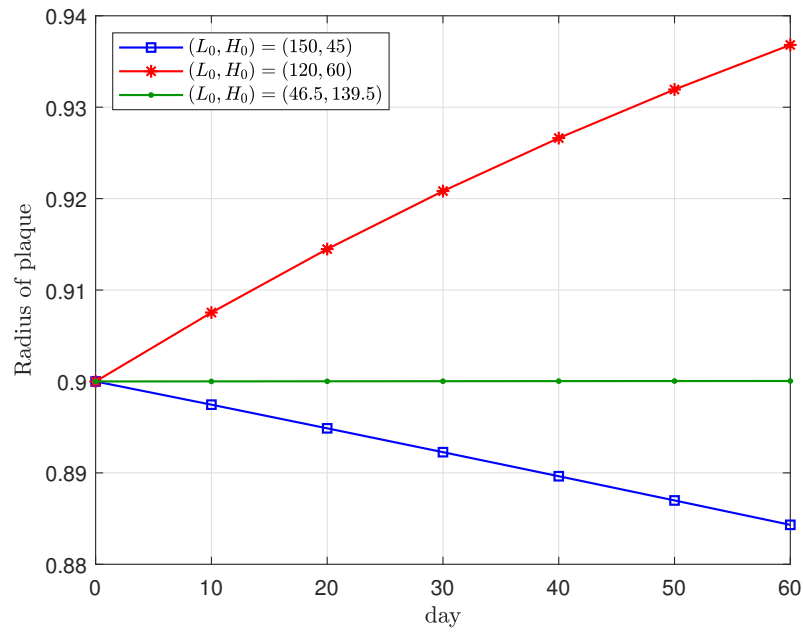**Table 8:** *Condition number of the coefficient ma-
trices.*

Fig. 11: *Variation of the radius of the plaque toward the various level of L_0 and H_0 in blood during the days.*
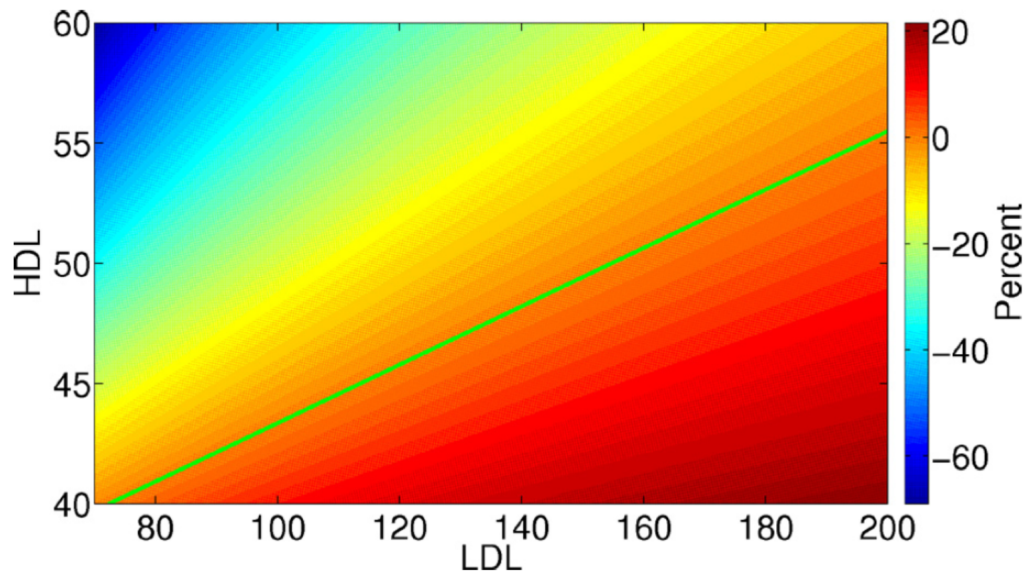

Fig. 12: *Risk Map. The values of LDL and HDL are measured in $mg/dl = 10^{-4}g/cm3$ [19].*
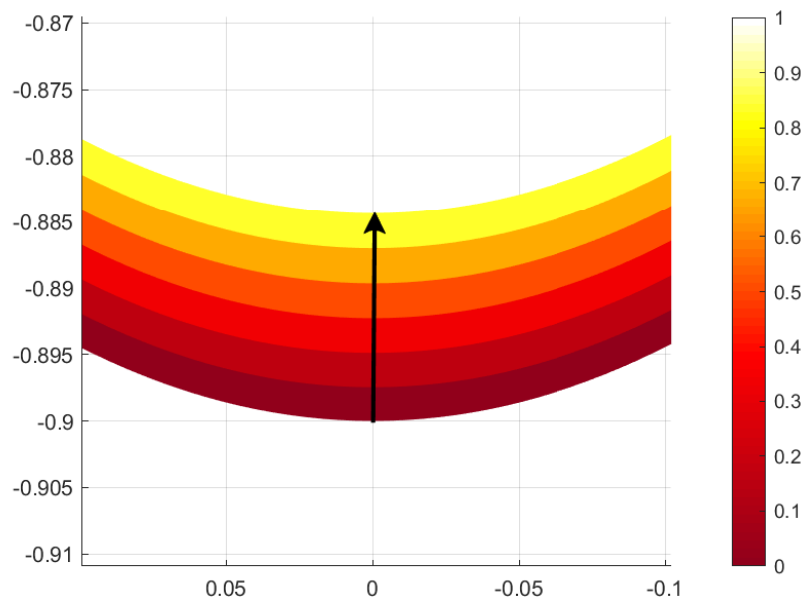
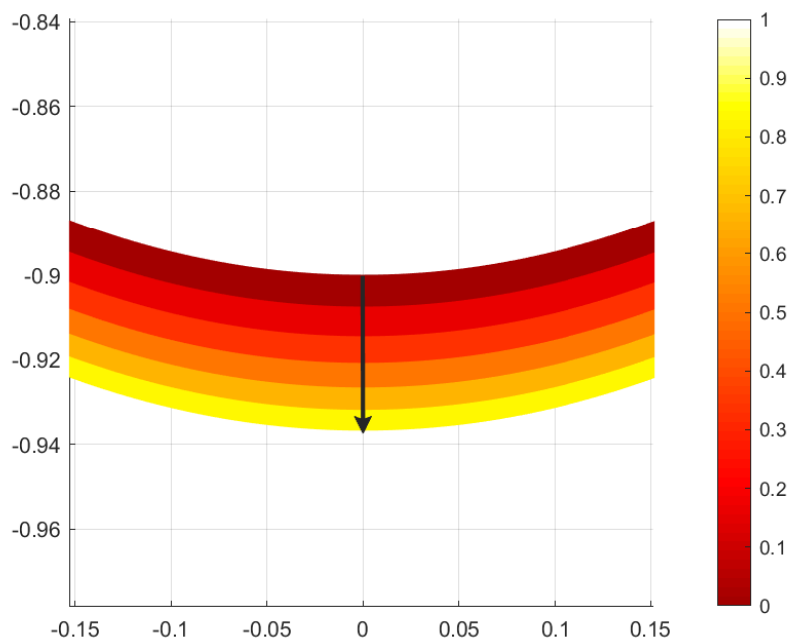**Fig. 13:** *Variation of the radius of the plaque with $L_0 = 150$ and $H_0 = 45$ in a small part of the artery.*

Fig. 14: *Variation of the radius of the plaque with $L_0 = 120$ and $H_0 = 60$ in a small part of the artery.*

(L_0, H_0)	0 day	10 day	20 day	30 day	40 day	50 day	60 day
$(150, 45)$	0.900000	0.897461	0.894874	0.892264	0.889634	0.886984	0.884316
$(120, 60)$	0.900000	0.907537	0.914481	0.920822	0.926622	0.931935	0.936810
$(46.5, 139.5)$	0.900000	0.900008	0.900018	0.900027	0.900037	0.900046	0.900055

Table 9: *Variation of the radius of the plaque toward the various level of L_0 and H_0 in blood during the days.*

7 Conclusion

There are many mathematical methods for solving biological models. However, mathematical modeling often produces nonlinear differential equations. Therefore, we cannot always obtain the exact solution of these equations; so, developing numerical techniques to solve these equations is required. In this study, a mathematical model of Atherosclerosis is solved numerically and the convergence and stability analysis are presented. For the readers convenience, we give the main contributions of this study as follows

• In this article, we use the front fixing method to convert the moving boundary problem (6)-(10) to a fix one (11)-(15), because classical numerical methods are not effective to solve free and moving boundary problems and moreover, because of the suitability of the front fixing method to apply to problems with regular geometries along with the mesh-based methods.

• To achieve more comfortable results for numerical analysis, we have simplified the model by changing the mix boundary condition of the equations (11)-(13) to a Neumann one by applying a suitable change of variables (17)-(18).

• To solve nonlinear systems, one way is to linearize the equations of the system and then, solve the linear one by classical methods. Since the model studied in this article is nonlinear, we have used Taylor theorem simultaneously both to linearize the equations and for constructing new second-order non-classical discretization formula to approximate time discretization (Finite difference method).

• In this article, we use spectral collocation method in space. To construct trial functions which satisfy the boundary conditions, the first way that comes to mind is to use a linear combination of monomial polynomials. But, there are some problems to use this kind of polynomials. some of these problems are as follows

1. The condition number of collocation matrices increases significantly by increasing the size of the matrices for $N \geq 10$ and because of that, we are limited to increase the collocation points and achieve arbitrary errors. (See Table 4 and Table 3)

2. The high error of collocation method affects the error of the finite difference method (See Table 1). To the above reasons, we use a linear combination of classical orthogonal polynomials or orthogonal functions to construct trial functions.

So, using orthogonal polynomials, the condition number of collocation matrices does not increase significantly by increasing the collocation points even for $N = 150$ (See Table 8, Figure 9 and Figure 10), and because of that, the error of the collocation method decreases compared to the TFBM case (See Table 7 and Figure 8).

• Moreover, the convergence and stability of the presented method is proved (See Theorem 5.2 and Theorem 5.3) and the order of convergence is presented. Numerical results in both TFBM and TFBL cases show that the finite difference method displays an $\mathcal{O}(h^2)$ order of convergence, as we expect from convergence Theorem 5.2 (See Figure 4 and Figure 7), and the space-error shows that using the collocation method, the results are converging to the exact solution.

• As illustrated in Figure 11 and Table 9, we present the effect of the level of L_0 and H_0 in blood on the growth and shrink of the plaque. It is easily can be seen that for $(L_0, H_0) = (150, 45)$ (below the "zero growth"), the plaque grows and for $(L_0, H_0) = (120, 60)$ (above the "zero growth") the plaque shrinks.

References

1. Inflammation in atherosclerotic plaque formation [video file] youtube; [cited 2013 jan 19]. retrieved from:. https://www.youtube.com/watch?v=Na6-kP9VYCU.

2. Alexander RA Anderson, Mark AJ Chaplain, E Luke Newman, Robert JC Steele, and Alastair M Thompson. Mathematical modelling of tumour invasion and metastasis. *Computational and mathematical methods in medicine*, 2(2):129–154, 2000.

3. DD Bankson, M Kestin, and N Rifai. Role of free radicals in cancer and atherosclerosis. *Clinics in laboratory medicine*, 13(2):463–480, 1993.

4. Jacob Fog Bentzon, Fumiyuki Otsuka, Renu Virmani, and Erling Falk. Mechanisms of plaque formation and rupture. *Circulation research*, 114(12):1852–1866, 2014.

5. Florian Cajori. The early history of partial differential equations and of partial differentiation and integration. *The American Mathematical Monthly*, 35(9):459–467, 1928.

6. Vincent Calvez, Abderrhaman Ebde, Nicolas Meunier, and Annie Raoult. Mathematical modelling of the atherosclerotic plaque formation. In *ESAIM: Proceedings*, volume 28, pages 1–12. EDP Sciences, 2009.

7. Vincent Calvez, Jean Gabriel Houot, Nicolas Meunier, Annie Raoult, and Gabriela Rusnakova. Mathematical and numerical modeling of early atherosclerotic lesions. In *ESAIM: Proceedings*, volume 30, pages 1–14. EDP Sciences, 2010.

8. Claudio Canuto, M Youssuff Hussaini, Alfio Quarteroni, and Thomas A Zang. *Spectral methods*. Springer, 2006.

9. Mark AJ Chaplain, Susan M Giles, BD Sleeman, and Richard J Jarvis. A mathematical analysis of a model for tumour angiogenesis. *Journal of mathematical biology*, 33(7):744–770, 1995.

10. Rebecca V Culshaw, Shigui Ruan, and Glenn Webb. A mathematical model of cell-to-cell spread of hiv-1 that includes a time delay. *Journal of mathematical biology*, 46(5):425–444, 2003.

11. Zhong-Shan Deng and Jing Liu. Mathematical modeling of temperature mapping over skin surface and its implementation in thermal disease diagnostics. *Computers in biology and medicine*, 34(6):495–521, 2004.

12. EH Doha, WM Abd-Elhameed, and YH Youssri. Fully legendre spectral galerkin algorithm for solving linear one-dimensional telegraph type equation. *International Journal of Computational Methods*, page 1850118, 2018.

13. Jens P Eberhard and Peter Frolkovic. Numerical simulation of growth of an atherosclerotic lesion with a moving boundary. 2006.

14. Sakine Esmaili and Mohammad Reza Eslahchi. Optimal control for a parabolic–hyperbolic free boundary problem modeling the growth of tumor with drug application. *Journal of Optimization Theory and Applications*, 173(3):1013–1041, 2017.

15. Sakine Esmaili and MR Eslahchi. Application of fixed point-collocation method for solving an optimal control problem of a parabolic–hyperbolic free boundary problem modeling the growth of tumor with drug application. *Computers & Mathematics with Applications*, 75(7):2193–2216, 2018.

16. Jennifer A Flegg, Helen M Byrne, Mark B Flegg, and DL Sean McElwain. Wound healing angiogenesis: the clinical implications of a simple mathematical model. *Journal of theoretical biology*, 300:309–316, 2012.

17. SJ Franks, HM Byrne, JR King, JCE Underwood, and CE Lewis. Modelling the early growth of ductal carcinoma in situ of the breast. *Journal of mathematical biology*, 47(5):424–452, 2003.

18. Avner Friedman and Wenrui Hao. A mathematical model of atherosclerosis with reverse cholesterol transport and associated risk factors. *Bulletin of mathematical biology*, 77(5):758–781, 2015.

19. Avner Friedman, Wenrui Hao, and Bei Hu. A free boundary problem for steady small plaques in the artery and their stability. *Journal of Differential Equations*, 259(4):1227–1255, 2015.

20. Walter Gautschi. *Numerical analysis*. Springer Science & Business Media, 1997.

21. Ross G Gerrity. The role of the monocyte in atherogenesis: I. transition of blood-borne monocytes into foam cells in fatty lesions. *The American journal of pathology*, 103(2):181, 1981.

22. Wenrui Hao and Avner Friedman. The ldl-hdl profile determines the risk of atherosclerosis: a mathematical model. *PloS one*, 9(3):e90497, 2014.

23. Godfrey Harold Hardy et al. Mendelian proportions in a mixed population. *Classic papers in genetics. Prentice-Hall, Inc.: Englewood Cliffs, NJ*, pages 60–62, 1908.

24. William Harvey. *Exercitatio anatomica de motu cordis et sanguinis in animalibus*, volume 2. 1737.

25. MJ Holmes and BD Sleeman. A mathematical model of tumour angiogenesis incorporating cellular traction and viscoelastic effects. *Journal of theoretical biology*, 202(2):95–112, 2000.

26. Can Huang, Zhimin Zhang, and Qingshuo Song. Spectral methods for substantial fractional differential equations. *Journal of Scientific Computing*, 74(3):1554–1574, 2018.

27. Md Hamidul Islam and Peter Johnston. A mathematical model for atherosclerotic plaque formation and arterial wall remodelling. *ANZIAM Journal*, 57:320–345, 2016.

28. E Javierre, FJ Vermolen, C Vuik, and S Van der Zwaag. A mathematical analysis of physiological and morphological aspects of wound closure. *Journal of mathematical biology*, 59(5):605–630, 2009.

29. Hassan Khosravian-Arab, Mehdi Dehghan, and MR Eslahchi. Generalized bessel functions: Theory and their applications. *Mathematical Methods in the Applied Sciences*, 40(18):6389–6410, 2017.

30. Mark P Little, Anna Gola, and Ioanna Tzoulaki. A model of cardiovascular disease giving a plausible mechanism for the effect of fractionated low-dose ionizing radiation exposure. *PLoS computational biology*, 5(10):e1000539, 2009.

31. Salvador E Luria and Max Delbrück. Mutations of bacteria from virus sensitivity to virus resistance. *Genetics*, 28(6):491, 1943.

32. EBS Marinho, Flora S Bacelar, and RFS Andrade. A model of partial differential equations for hiv propagation in lymph nodes. *Physica A: Statistical Mechanics and its Applications*, 391(1-2):132–141, 2012.

33. Mark M Meerschaert. *Mathematical modeling*. Academic press, 2013.

34. Isaac Newton. Methodus fluxionum et seriarum infinitarum. *Opuscula mathematica, philosophica et philologica*, 1, 1774.

35. World Health Organization. *International statistical classification of diseases and related health problems*, volume 1. World Health Organization, 2004.

36. Anna Ougrinovskaia, Rosemary S Thompson, and Mary R Myerscough. An ode model of early stages of atherosclerosis: mechanisms of the inflammatory response. *Bulletin of mathematical biology*, 72(6):1534–1561, 2010.

37. R Owen and Jonathan A Sherratt. Mathematical modelling of macrophage dynamics in tumours. *Mathematical Models and Methods in Applied Sciences*, 9(04):513–539, 1999.

38. Salomonsky Paul-Michael. A mathematical system for human implantable wound model studies. 2013.

39. Mehdi Ramezani, Mehdi Dehghan, and Mohsen Razzaghi. Combined finite difference and spectral methods for the numerical solution of hyperbolic equation with an integral condition. *Numerical Methods for Partial Differential Equations: An International Journal*, 24(1):1–8, 2008.

40. R Rockne, EC Alvord, JK Rockhill, and KR Swanson. A mathematical model for brain tumor response to radiation therapy. *Journal of mathematical biology*, 58(4-5):561, 2009.

41. Hermann Schichl. Models and the history of modeling. In *Modeling languages in mathematical optimization*, pages 25–36. Springer, 2004.

42. David M Seo, Pascal J Goldschmidt-Clermont, Mike West, et al. Of mice and men: Sparse statistical modeling in cardiovascular genomics. *The Annals of Applied Statistics*, 1(1):152–178, 2007.

43. Jie Shen, Tao Tang, and Li-Lian Wang. *Spectral methods: algorithms, analysis and applications*, volume 41. Springer Science & Business Media, 2011.

44. Randhir Singh, Sushma Devi, and Rakesh Gollen. Role of free radical in atherosclerosis, diabetes and dyslipidaemia: larger-than-life. *Diabetes/metabolism research and reviews*, 31(2):113–126, 2015.

45. Angélique Stéphanou, Steven R McDougall, Alexander RA Anderson, and Mark AJ Chaplain. Mathematical modelling of the influence of blood rheological properties upon adaptative tumour-induced angiogenesis. *Mathematical and Computer Modelling*, 44(1-2):96–123, 2006.

46. Emmanuelle Terry, Jacqueline Marvel, Christophe Arpin, Olivier Gandrillon, and Fabien Crauste. Mathematical model of the primary cd8 t cell immune response: stability analysis of a nonlinear age-structured system. *Journal of mathematical biology*, 65(2):263–291, 2012.

47. Yifan Yang, Willi Jäger, Maria Neuss-Radu, and Thomas Richter. Mathematical modeling and simulation of the evolution of plaques in blood vessels. *Journal of mathematical biology*, 72(4):973–996, 2016.

48. Ge Yule. *The growth of population and the factors which control it*. Harrison & Sons, 1925.

49. Yanmin Zhao, Yadong Zhang, Fawang Liu, I Turner, Yifa Tang, and V Anh. Convergence and superconvergence of a fully-discrete scheme for multi-term time fractional diffusion equations. *Computers & Mathematics with Applications*, 73(6):1087–1099, 2017.